의학박사 학위논문

세포외소포체 분석을 통한 난소암 진단 및 전이 조절 연구

The role of extracellular vesicles in ovarian cancer diagnosis and metastasis regulation

2022년 8월

서울대학교 대학원

의과대학 협동과정 종양생물학 전공

Wenyu Wang

세포외소포체 분석을 통한 난소암 진단 및 전이 조절 연구

지도 교수 송용상

이 논문을 의학박사 학위논문으로 제출함

2022년 4월

서울대학교 대학원

의과대학 협동과정 종양생물학 전공

원위

원위의 의학박사 학위논문을 인준함

2022년 7월

위 원 장 _____ (인)

부위원장 _____ (인)

위 원 _____ (인)

위 원 _____ (인)

위 원 _____ (인)

The role of extracellular vesicles in ovarian cancer diagnosis and metastasis regulation

Wenyu Wang
(Directed by Yong Sang Song, M.D., Ph.D.)
Submitting a Ph.D. Dissertation of
Interdisciplinary Graduate Program in
Cancer Biology

April 2022

College of Medicine
Seoul National University
Interdisciplinary Graduate Program in
Cancer Biology

Wenyu Wang

Confirming the Ph.D. Dissertation written by
Wenyu Wang
July 2022

Chair _____(Seal)
Vice Chair _____(Seal)
Examiner _____(Seal)
Examiner _____(Seal)
Examiner _____(Seal)

Abstract

Ovarian cancer is mostly diagnosed at advantaged stages due to the lack of early diagnostic biomarkers. The common metastasis pattern is characterized by peritoneal dissemination with a formation of malignant ascites. Extracellular vesicles (EVs) are emerging as promising clinical biomarkers in liquid biopsy. Here, we aimed to investigate robust liquid biopsy-based EV miRNA biomarkers for ovarian cancer diagnosis and metastasis regulation. EVs were isolated from malignant ascites and plasma of ovarian cancer patients as well as the benign control counterparts of patients with benign gynecologic diseases. Small RNA sequencing was carried out investigating the miRNA profiling of ascites- and plasma-derived EVs. Eight miRNAs (miR-1246, miR-1290, miR-483, miR-429, miR-34b-3p, miR-34c-5p, miR-145-5p, miR-449a) were selected based on dysregulated miRNAs overlapped in the ascites and plasma subset to develop the ovarian cancer EV miRNA (OCEM) signature. The ovarian cancer EV miRNA (OCEM) signature of these eight miRNAs demonstrated a high diagnostic accuracy in our in-house dataset (ascites subset: AUC=1; plasma subset: AUC=0.9375). This diagnostic signature also demonstrated high diagnostic accuracy in multiple public datasets across diverse clinical samples (blood, tissue

and urine). In addition, the impact of malignant ascites-derived EVs on the malignant behaviors of ovarian cancer cells was also assessed. The result showed that malignant ascites-derived EVs could significantly facilitate the metastatic potential of ovarian cancer cells. Notably, miR-1246 and miR-1290 shuttled in malignant ascites-derived EVs were identified to promote the invasion and migration of ovarian cancer cells by regulating a common target RORα. Our study highlights that the EV miRNA signature shows great promise as a clinically applicable liquid biopsy strategy for ovarian cancer diagnosis. In addition, malignant ascites-derived EVs could significantly promote the cancer metastatic potential through delivering oncogenic miRNAs, serving as a potential therapeutic target for ovarian cancer management.

Keywords: Ovarian cancer, extracellular vesicles, miRNA, ascites, liquid biopsy, diagnosis, metastasis

Student Number: 2018-36129

Graphic abstract

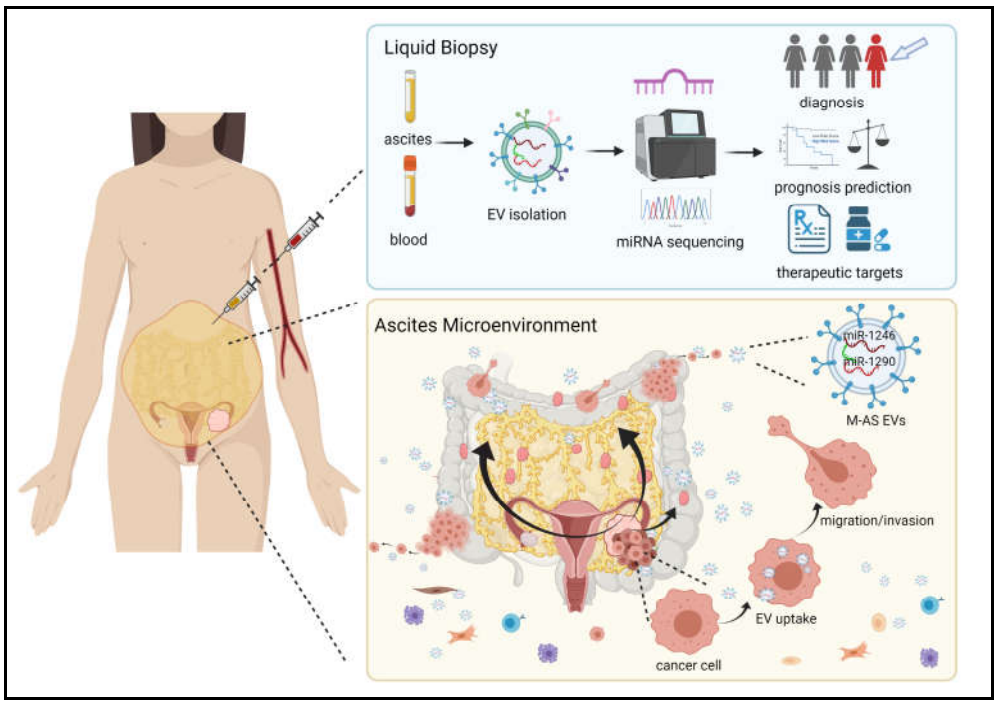

Table of Contents

List of Tables and Figures

Chapter 1. Literature review: Non-coding RNAs shuttled via exosomes reshape the hypoxic tumor microenvironment

Chapter 2. Integrated analysis of ascites and plasma extracellular vesicles identifies a panel of miRNAs for ovarian cancer diagnosis

Chapter 3. Malignant ascites-derived EVs facilitate the invasion and migration of ovarian cancer cells through transferring miR-1246 and miR-1290

Abbreviations:

miRNAs: MicroRNAs

lncRNAs: Long non-coding RNAs

miRISC: MiRNA-induced silencing complex

EVs : Extracellular vesicles

ROS: Reactive oxygen species

ECM: Extracellular matrix

HIF-1: Hypoxia-inducible factor-1

PHD: Prolyl hydroxylase

VHL: Von Hippel-Lindau

PD-1: Programmed cell death protein 1

PD-L1: Programmed death-ligand 1

MDSC: Myeloid-derived suppressor cell

CAF: Cancer-associated fibroblast

IGF1: Insulin-like growth factor 1

MVBs: Multi-vesicular bodies

ESCRT: Endosomal-sorting complex required for transport

NK cell: Natural killer cell

PDGF: Platelet-derived growth factor

BMSC: Bone marrow-derived mesenchymal stem cell

TAM: Tumor-associated macrophage

Treg: Regulatory T cell

DC: Dendritic cell

CTLA-4: Cytotoxic T-lymphocyte antigen 4

iNOS: Inducible nitric oxide synthase

EGF: Epidermal growth factor

EMT: Epithelial-mesenchymal transition

HREs: Hypoxic response elements

NPC: Nasopharyngeal carcinoma

GBM: Glioblastoma multiforme

EOC: Epithelial ovarian cancer

OSCC: Oral squamous cell carcinoma

HCC: Hepatocellular carcinoma

NSCLC: Non-small-cell lung cancer

HGSOC: high-grade serous ovarian cancer

CTCs: circulating tumor cells

ctDNAs: circulating tumor DNAs

NTA: nanoparticle tracking analysis

TEM: transmission electron microscopy

IHC: immunohistochemistry

MA-EVs: malignant ascites-derived EVs

BA-EVs: benign peritoneal fluid-derived EVs

MP-EVs: malignant plasma-derived EVs

BP-EVs: benign plasma-derived EVs

DEmiRs: differentially expressed miRNAs

OCEM signature: ovarian cancer EV miRNA signature

ROC curve: receiver operating characteristic curve

AUC: area under the curve

miRNA IN: miRNA inhibition

miRNA OV: miRNA overexpression

RORα: retinoid orphan receptor alpha

CRISPR/Cas9: Clustered Regularly Interspaced Short Palindromic Repeats/CRISPR-associated protein 9

Chapter 1.

Literature review: Non-coding RNAs shuttled via exosomes reshape the hypoxic tumor microenvironment

1. Background

Cancer cells persistently interact with other cell types in the tumor microenvironment. Cells cohabiting in a tumor niche are affected significantly by surrounding factors (1). Low oxygen status, termed as hypoxia, is one of the most important characteristics of solid tumors. Hypoxia can elicit fundamental changes in cancer cells and affect cell-to-cell communications. Autocrine and paracrine signaling through cytokines and chemokines have been studied intensively in molecular oncology for the last decades (2, 3). Emerging studies suggest exosomes secreted by different cell types are actively involved in modulating cancer cell phenotypes and dictating cancer hallmarks.

Exosomes contain cytosolic cargos of donor cells, assisting the membrane-protected cargos to travel a long distance. Among many other cytosolic cargos found in exosomes, non-coding RNAs(ncRNAs) including micro RNAs (miRNAs), long non-coding RNAs (lncRNAs) and circular RNAs (circRNAs) are most intensively studied in that

they act as vital regulators in transcriptional and post-transcriptional levels. Investigating the effects of exosomal non-coding RNAs in the hypoxic tumor microenvironment is critical to elucidate the key underlying mechanisms of cancer progression.

1.1 Tumor microenvironment and hypoxia

Accumulative evidence suggests that tumor cells behave differently depending on extrinsic factors of the surrounding microenvironment. Distinct types of cells including immune cells, fibroblasts and endothelial cells interactively communicate to facilitate cancer progression (4). Additionally, pH, reactive oxygen species (ROS), inflammation, components in the extracellular matrix (ECM) and hypoxia can influence the metabolism and aggressiveness of cancer (5-8). Therefore, the various interplay between cellular and non-cellular factors in the tumor microenvironment may serve as potential therapeutic targets in the clinical settings.

Irregular vessel formation and the rapid proliferation of cancer cells create hypoxic conditions in malignant tumors. In this regard, hypoxia is a common feature in the microenvironment of most solid tumors (9). Clinical studies have revealed that overexpression of hypoxia-induced genes is associated with poor prognosis in many cancer types including pancreatic, lung, breast, prostate and ovarian cancer (10-14). Besides, plentiful in vitro and in vivo experimental

data have suggested that hypoxia orchestrates malignant phenotypes of cancer cells through activation of multiple oncogenic signaling pathways. Transcription factors and epigenetic regulators can concertedly exert reinforcement of oncogenic signaling pathways, controlling the expression of numerous genes under hypoxia. Nevertheless, interactions between cancerous cells and non-cancerous cells could be further invigorated in the hypoxic tumor microenvironment. Cancer cells stimulated by hypoxia manifest increased drug-resistance, tumorigenesis, angiogenesis, invasiveness and immune suppression (15).

Several decades ago, oxygen sensing mechanisms at the molecular level had been discovered that some transcription factors play a central role in tissues in response to low oxygen tension (<10 mmHg) (16). The vital proteins involved in the process of cellular adaptation under hypoxia are: hypoxia-inducible factor-1 (HIF-1), prolyl hydroxylase (PHD) and von Hippel-Lindau (VHL). HIF-1α is a transcription factor constitutively activated in response to hypoxia (17). Under normal oxygen tension (45-65 mmHg) at peripheral tissues, PHD is activated, adding a hydroxyl group to HIF-1α at a proline residue. Hydroxylated HIF-1α is then subjected to degradation through ubiquitination, mediated by the VHL complex. Unlike HIF-1α, its binding partner, HIF-1β is stably expressed

even at the high oxygen tension. Under hypoxic conditions, the accumulated dimer of HIF-1α and HIF-1β bind to hypoxic response elements (HREs) of various genes in the nucleus. Activated HREs are closely associated with oncogenic phenotypes such as proliferation, invasion, epithelial-mesenchymal transition (EMT) and metabolic reprogramming (16). Furthermore, recent studies have illustrated that myriad epigenetic modifications are involved in hypoxic signals through histone modifications and DNA methylation (18, 19).

The hypoxic conditions also affect interactions between cancerous and non-cancerous cells in the tumor microenvironment. Hypoxia-induced overexpression of programmed death-ligand 1 (PD-L1) in cancer cells, disabling cytotoxic functions of programmed cell death protein 1 (PD-1) positive activated T lymphocytes (20, 21). Moreover, HIF-1α promoted the overexpression of PD-L1 in myeloid-derived suppressor cells (MDSCs) and macrophages, neutralizing anti-cancer immunity in the tumor microenvironment (22). Additionally, hypoxia upregulated V-domain Ig suppressor of T-cell activation (VISTA) in MDSCs, thereby suppressing T cell activity (23). CD47 enriched at the plasma membrane of hypoxic tumors inhibited the phagocytic activity of macrophages (23, 24). Along with hypoxia-induced changes in the tumor immune microenvironment, hypoxia can assist tumor growth by

reprogramming fibroblasts. In the study which utilized the cancer-associated fibroblast (CAF)-endothelial cell co-culture model, hypoxic CAFs promoted angiogenesis through NCBP2-AS2 mediated vascular endothelial growth factor A (VEGFA) secretion (25). In line with the result from the CAF-endothelial co-culture study, another study demonstrated that CAF induced angiogenesis via recruitment of HIF-1α and G-protein estrogen receptor (GPER) to the promoter region of VEGF (26). Moreover, pancreatic CAFs produced more insulin-like growth factor 1 (IGF1) and cancer cells increased the expression of IGF1 receptor (IGF1R) in response to hypoxia. This specific hypoxia-potentiated CAF-cancer cell communication promoted the metastatic ability of pancreatic cancer cells (27). A multi-center study from Norwegian hospitals suggested that upregulation of miRNA-210, a hypoxia-induced miRNA, in CAFs but not in cancer cells was negatively correlated with the prognosis of prostate cancer patients (28). Therefore, hypoxic responses of both cancerous and non-cancerous cells are vital determining factors of cancer progression.

Transcriptomic and epigenetic landscapes of a tumor are vastly changed by hypoxia. As recent studies have underscored the importance of exosomes as a critical mode of cell-to-cell communication, it would be worthwhile to unveil how exosomal non-

coding RNA signaling regulates the hypoxic tumor microenvironment.

1.2 Exosomes and non-coding RNAs

Extracellular vesicles (EVs) are secreted by almost all cell types into the extracellular space. EVs are classified into microvesicles, apoptotic bodies, exosomes, etc. according to their intracellular origin, size, and biogenesis (29). Exosomes are endogenous vehicles with a size of 40-150 nm in diameter. Endocytic vesicles produced in the plasma membrane can form early-endosomes by continuous endocytosis and develop into late-endosomes. Late-endosomes bud inwards to form multi-vesicular bodies (MVBs), and the fused MVBs with the plasma membrane enables the release of intraluminal vesicles (ILVs) into extracellular space, called exosomes (30). The endosomal-sorting complex required for transport (ESCRT) machinery is necessary for exosome formation at endosomes. It is complicated protein machinery comprised of four proteins ESCRTs (0 through III) regulating MVB formation, vesicle budding, and cargo sorting (31). However, some studies have revealed an ESCRT-independent exosomal cargo sorting manner, suggesting that the mechanisms are broader and more intricate.

Exosomes are mediators of cell-cell interactions in that they are capable of delivering functional mRNAs, microRNAs (miRNAs), DNAs, and proteins to recipient cells altering their physiological and

pathological functions. These exosomal cargos are enclosed inside the double membrane and are stable to environmental factors such as nucleases, proteases and oxidative stress so that they can be delivered to recipient cells in an efficient and intact manner (32, 33). Cancer cell-derived exosomes affect cancer progression such as proliferation, drug resistance, and metastasis (34). Meanwhile, these tumor-derived exosomes also have a significant impact on various stromal cells in the tumor microenvironment. They are involved in the function of endothelial cells, the polarization of macrophages, regulation of T cells, and suppression of natural killer cells (NK cells) activity and other biological activities (35-38). Stromal cell-secreted exosomes, in turn, can support the malignant phenotypes of cancer cells. For instance, tumor-associated macrophage (TAM)-derived exosomes containing functional factors promoted migration and invasion in breast cancer (39). CAF-derived exosomes conferred chemoresistance to ovarian cancer cells (40). Therefore, exosomes may play a pivotal role in the inter-tumor cell, inter-stromal cell and tumor-stromal cell interactions.

Additionally, exosomes have been detected in almost all types of body fluids such as blood, urine, saliva, breast milk, and ascites. They can be used as biomarkers to diagnose diseases in non-invasive or minimally invasive ways (41). Furthermore, exosomes

can be used as natural nano-carriers for therapeutic applications that can efficiently deliver various signaling molecules. Exosomes show similar structures to a bilayer of lipids of cell membranes because they fuse to the plasma membrane during secretion. Recent researches have shown the possibility that exosome-mediated delivery of small interfering RNAs (siRNAs), antioxidants, anticancer drugs, and CRISPR/Cas9 system via low immunogenicity (42-45).

RNAs are classified into protein-coding RNAs and non-coding RNAs according to their protein-coding abilities. Based on the Francis Crick's 'the central dogma of molecular biology', many studies have focused on processes of protein production through messenger RNA (mRNA), and constituent RNAs such as ribosomal RNAs (rRNAs) or translators of codon sequence (tRNA) (46, 47). However, results from human genome sequencing found that only ~200,000 RNAs could encode proteins, comprising only 2% of the genomes (48). In 1965, scientists discovered a new type of regulatory non-coding RNAs that do not function through protein translation (49). Non-coding RNAs are divided based on the number of nucleotides constituting the RNAs: small non-coding RNAs including miRNAs, siRNAs, piwi-interacting RNAs (piRNAs) composed of less than 200 nucleotides and lncRNAs with more than 200 nucleotides in size (50). In addition, another type of non-coding

RNAs highly represented in the eukaryotic transcriptome is circRNAs, which form covalently closed continuous loop structures, unlike the above-mentioned linear RNAs. CircRNAs are relatively stable compared to linear non-coding RNAs. Exosomes contain a variety of RNA species, among which miRNAs are the most abundant and surely most intensively studied while lncRNAs and circRNAs are also becoming research hotspots now. Some qualitative and quantitative assays have revealed the asymmetric distribution of RNAs between cells and cell-derived exosomes. This phenomenon has boosted many interesting hypotheses, suggesting that RNA molecules are not randomly packaged in exosomes but with a set of sorting systems involved.

A single mammalian cell carries approximately 100,000 endogenous miRNAs, while a single exosome contains about 500 miRNAs. Pigati et al. found that the abundance of about 66% of extracellular miRNAs well reflected the corresponding abundance of miRNAs in the cells (51). Van Balkom et al. also reported that the most abundant exosomal miRNAs closely corresponded with the most abundant cellular miRNAs (52). These findings suggest that the majority of high expressed miRNAs are encapsulated and secreted via exosomes passively for an osmotic-like effect. However, there was still a category of miRNAs that might be selectively retained or

released. For example, more than 90% of the mature miR-451, which is functioned as a tumor suppressive gene in breast cancer, was found to be exported into extracellular space (52). In addition, Hannafon et al. observed that miR-451, miR-122, miR-1246, miR-21 were more enriched in the breast cancer cell-derived exosomes than normal epithelial cell-derived exosomes. Intriguingly, oncogenic miR-1246 and miR-21 showed consistent high abundancy in the cells while tumor suppressive miR-451 and miR-122 were downregulated in cellular expression (53). Based on these studies, it can be inferred that apart from the passive osmotic-like pattern, the function-dependent selective mechanism may be present when RNAs are secreted via exosomes. Cells might tend to secrete RNAs that are unnecessary, advantageous or even harmful for sustaining cell properties. Ragusa et al. further strengthened and developed this point. They found that in addition to tumor suppressive miRNAs, immunosuppressive miRNAs were also highly abundant in exosomes compared to cells, which indicated that RNAs might be selectively released into the tumor microenvironment to influence the immune response (54).

Some lipids and proteins have been demonstrated to be involved in sorting specific non-coding RNAs into exosomes. The neural sphingomyelinase 2 (nSMase2) was reported to be associated with

the secretion of exosomes, which was also the first molecule found to guide miRNAs into exosomes. The expression of nSMase2 was positively related to the level of exosomal miRNAs (55). Besides, some important proteins might also impact the RNA selective sorting process. Argonaute 2 (Ago2), a component of the miRNA-induced silencing complex (miRISC), was implicated in the assortment of several miRNAs into exosomes. Additionally, Alix, an accessory protein of ESCRT, was reported to be involved in the release of exosomal miRNAs from liver stem-like cells through interacting with Ago 2 (56). It has been reported that hypoxia could inhibit the Ago2 degradation by mediating hydroxylation of Ago2 by C-P4H(I) and increase the various functions of it, indicating the possible regulative role of hypoxia in sorting miRNAs into exosomes (57). Villarroya-Beltri et al. identified that some short motifs were overexpressed in exosomal miRNAs and mRNAs. The protein heterogeneous nuclear ribonucleoprotein A2B1 (hnRNPA2B1) could bind to those motifs and modulate RNAs loading into exosomes. Moreover, this process was controlled by the sumoylation of hnRNPA2B1 (58). Besides, hnRNPA2B1 was also reported to be involved in the encapsulation of lncARSR into exosomes (59). Kossinova et al. detected several structural motifs enriched in exosomal lncRNAs and mRNAs using bioinformatics approaches. Cytosolic Cold shock protein YB-1 and

RNA methyltransferase NSUN2 could recognize these motifs and mediate sorting specific lncRNAs and mRNAs into exosomes (60). YB-1 was reported to be physically interacted with HIF-1α and regulate the transcription of hypoxia-dependent genes (61). In addition, YB-1 could enhance the expression of HIF-1α and promote the invasion and metastasis in sarcoma (62). Li et al. showed more abundant circRNAs were present in exosomes compared to the source cells by RNA-sequencing analyses for the first time. The level of exosomal circRNAs and cellular circRNAs were only moderately correlated, suggesting that certain circRNAs might be actively incorporated into exosomes while some might be selectively retained in cells. CircRNAs have been reported to be capable of binding to miRNAs working as miRNA sponges. The authors also demonstrated that the selective sorting of circRNAs was associated with the relevant miRNAs (63). Overall, non-coding RNAs with certain sequences may favor themselves loading into exosomes whereas a bunch of protein complexes or lipids might be involved as well. However, there is still a lack of ample evidence that fully illustrates the underlying mechanism of the RNA sorting process and further investigations are deserved.

1.3 Hypoxia alters exosome release and exosomal components

Hypoxia can activate various pathways to promote the secretion

of exosomes and alter the components loaded in exosomes (Figure 1). Rab GTPases such as Rab27a and Rab27b are essential for exosomal secretion pathways in cancer cells (64). In hypoxic conditions, altered protein expression of small GTPase in cells promotes endocytosis, consequently changing the degree of exosomal secretion (65). In ovarian cancer, hypoxia significantly promoted exosome secretion though the upregulation of Rab27a. These hypoxia-induced exosomes elicited a more aggressive and chemoresistant phenotype of cancer cells (66). King et al. also confirmed that hypoxic breast cancer cells produced a higher level of exosomes in a HIF-1α-dependent manner (67). Rab5 could regulate vesicle-mediated transportation from the cell membrane to early endosomes and early endosome fusion (68). Under hypoxia, Rab5 was clustered in the perinuclear region while CD63 showed higher co-localization with the actin cytoskeleton of prostate cancer cells, suggesting that hypoxia could enhance exosome secretion through promoting early endosome formation and fusion of multivesicular endosomes with the plasma membrane (69).

The hypoxic conditions not only boost the release of exosomes but also influence the molecules contained within exosomes. Hypoxia-induced exosomes exhibit different patterns of various molecules depending on origin cells and environmental factors. In

highly malignant brain tumor glioblastoma multiforme (GBM), hypoxic cancer cell-derived exosomes showed enrichment in hypoxia-associated mRNAs and proteins (e.g., matrix metalloproteinases, IL-8, platelet-derived growth factor (PDGF), caveolin 1, and lysyl oxidase) and activated vascular cells in a hypoxia-dependent mode during cancer progression (70). Recent studies have shed light on the exosomal non-coding RNA expression and function shift in the hypoxic tumor microenvironment. Especially with the development of sequencing technology, more and more significant non-coding RNAs are being uncovered. It has been reported that miR-21, miR-23a, lncRNA-UCA1 were upregulated in the exosomes derived from hypoxic cancer cells and promoted cancer progression in various signaling pathways (71-73). Hypoxia was also reported to regulate the expression of circRNAs. Boeckel et al. first identified that cZNF292, cAFF1 and cDENND4C were upregulated while cTHSD1 was under the hypoxic condition in endothelial cells. Moreover, cZNF292 exhibited proangiogenic activities in vitro (74). While in cancer, hypoxia could induce the expression of circDENND2A, which could promote the migration and invasion of glioma cells through sponging miR-625-5p (75). The expression of circHIPK3 was reported to be upregulated in hypoxic exosomes compared with normoxic exosomes derived from cardiomyocytes. It could regulate

the oxidative damage in cardiac microvascular endothelial cells by inducing miR-29a/IGF-1 signaling pathway (76). This is the only report by now focusing on circRNAs in hypoxic exosomes. There is no direct evidence showing the role of hypoxic exosomal circRNAs in cancer yet. Collectively, Non-coding RNAs have been reported to exert various functions in translation, RNA splicing, DNA replication, etc. (71, 77-79). Further investigations are warranted to comprehensively understand the role of non-coding RNAs in the tumor microenvironment.

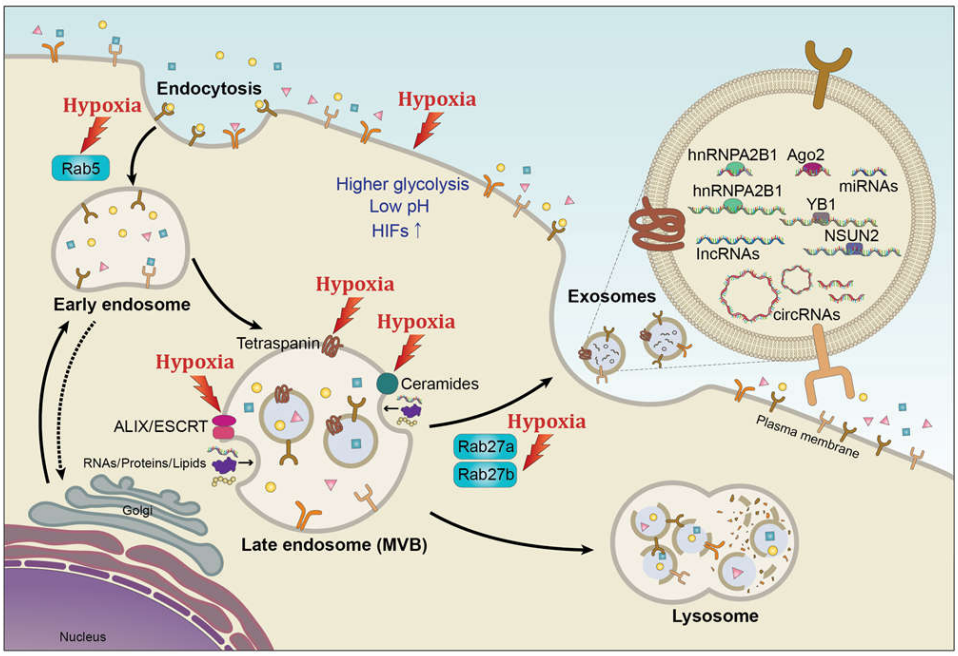
Hypoxia
Endocytosis
Hypoxia
Rab5
Higher glycolysis
Low pH
HIFs ↑
Early endosome
Hypoxia
Hypoxia
Tetraspanin
Hypoxia
Ceramides
ALIX/ESCRT
RNAs/Proteins/Lipids
Hypoxia
Rab27a
Rab27b
Golgi
Late endosome (MVB)
Nucleus
Exosomes
hnRNPA2B1
Ago2
hnRNPA2B1
miRNAs
YB1
NSUN2
lncRNAs
circRNAs
Plasma membrane
Lysosome

Figure 1. Hypoxia influences the secretion and non-coding RNA cargos of exosomes

Extracellular components enter cells through endocytosis along with the plasma membrane, leading to the formation of early endosomes and late endosomes (MVBs). Some molecules like ESCRT machinery, ALIX, tetraspanins and ceramides are involved in this process. Several Rab GTPases are associated with MVBs transporting to the plasma membrane. Then exosomes with specific cargos are released through exocytosis. Hypoxia triggers the alteration in gene expression of HIFs or other signaling pathways, which may impact exosome biogenesis and cargo sorting by regulating these molecules. Besides, non-coding RNAs binding with some RNA binding proteins like hnRNPA2B1, YB1, NSNU2 or Ago2 might be favorably sorted into exosomes.

2. Effects of hypoxic exosomal non-coding RNAs in the tumor microenvironment

Exosomes derived from hypoxic cancer cells or stromal cells play a fundamental role in the tumor microenvironment through transmitting non-coding RNAs. Hypoxia-induced exosomal non-coding RNAs have been demonstrated to regulate cancer proliferation, metastasis, chemoresistance, immune response and angiogenesis, thus reshaping the microenvironment (Figure 2).

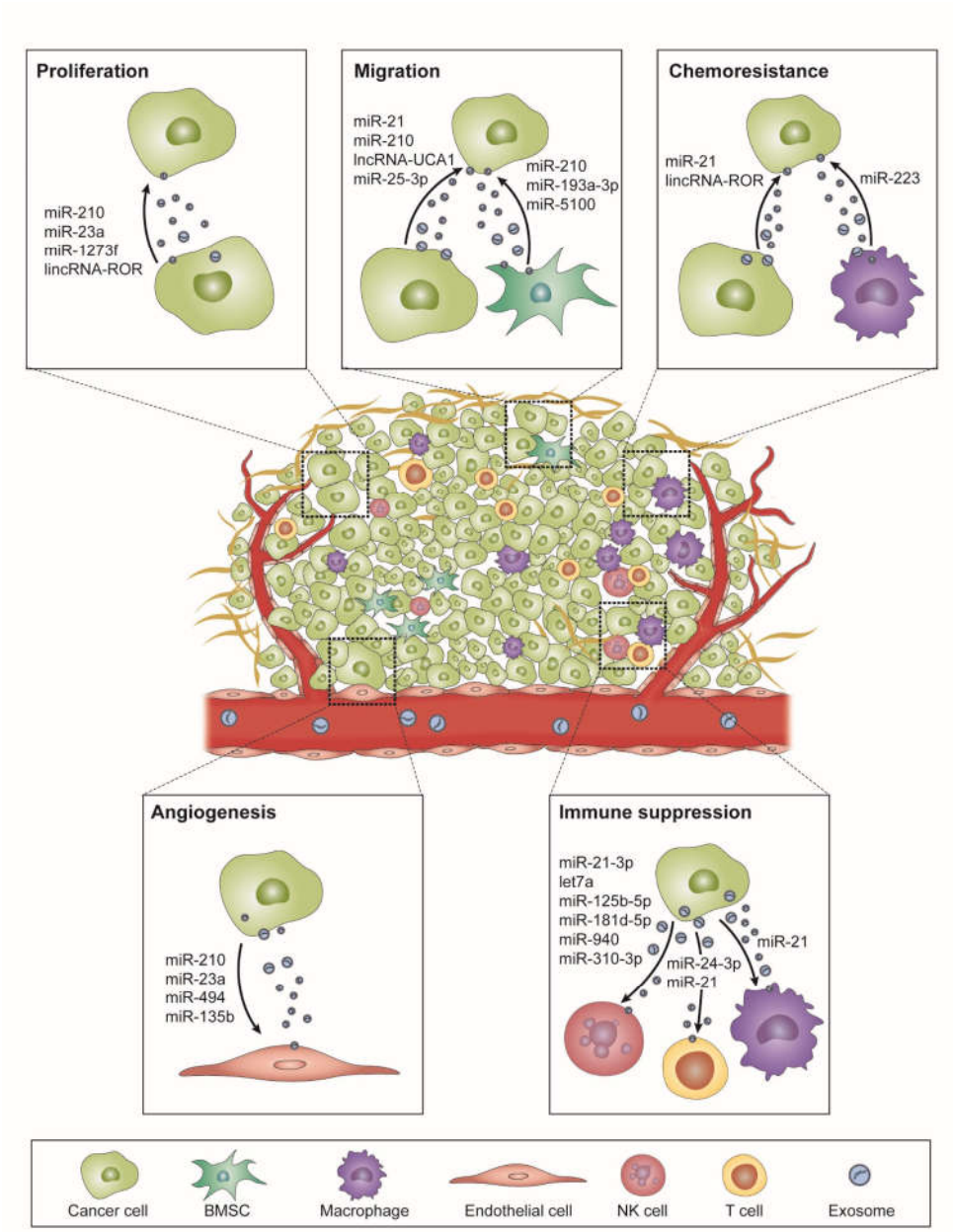
Proliferation
miR-210
miR-23a
miR-1273f
lincRNA-ROR
Migration
miR-21
miR-210
lncRNA-UCA1
miR-25-3p
miR-210
miR-193a-3p
miR-5100
Chemoresistance
miR-21
lincRNA-ROR
miR-223
Angiogenesis
miR-210
miR-23a
miR-494
miR-135b
Immune suppression
miR-21-3p
let7a
miR-125b-5p
miR-181d-5p
miR-940
miR-310-3p
miR-24-3p
miR-21
miR-21
Cancer cell
BMSC
Macrophage
Endothelial cell
NK cell
T cell
Exosome

Figure 2. Exosomal non-coding RNAs regulate the hypoxic tumor microenvironment

Hypoxic donor cells impact recipient cells by transmitting non-coding RNAs via exosomes. These exosomal non-coding RNAs can be uptaken by recipient cells and alter their biological behaviors through various pathways, thus regulating tumor development.

2.1 Proliferation

Hypoxia alters tumor metabolism and transcription such as a shift to glycolysis and self-sufficient release of growth signals (80). Even though much has been known about hypoxia-secreted metabolites promote tumor growth, the importance of hypoxic exosome-mediated tumor growth has been recently grown. Accumulating evidence indicates that pro-tumorigenic molecules secreted through exosomes in the hypoxic tumor microenvironment can promote tumor cell survival and proliferation.

MiR-210 is a well-recognized hypoxia-induced miRNA involved in various biological processes of cancer progression. It was reported to be upregulated in many types of solid tumors and related to unfavorable clinical outcomes of patients (81). In breast cancer, miR-210 was significantly elevated in the exosomes derived from hypoxic cancer cells than those from normoxic ones (67). Tang et al. utilized a breast cancer cell spheroid culture model to enrich highly malignant breast cancer stem cells (BCSCs). They corroborated that miR-210 was remarkably upregulated in hypoxic spheroid cells and spheroid-derived BCSCs compared to parental cells. The upregulation of miR-210 promoted the proliferation, self-renewal and migration of BCSCs (82). Furthermore, Yu et al. reported that miR-1273f upregulated in hypoxic tumor-derived exosomes

promoted cancer proliferation of hepatocellular carcinoma (HCC) by inhibiting LHX6/Wnt/β-catenin pathway (83). In another research of HCC, Patel and his colleagues showed that hypoxic tumor-derived exosomes reduced cancer cell viability with the increased expression of lncRNA-RoR. Knockdown of lncRNA-ROR induced expression of its target, miR-145, thus decreasing p70S6K1 (RPS6KB1) phosphorylation, PDK1 and HIF-1α expression (84). Wozniak et al. identified a set of differentially expressed exosomal miRNAs in hypoxic conditions. Hypoxia upregulated miR-494-5p, miR-4497, miR-513a-5p, miR-6087 while downregulating miR-125b-5p, miR-21-5p, miR-3934-5p in the exosomes from patient-derived melanoma cell lines cultured under hypoxia. Pathway analysis with bioinformatical tools has shown that these miRNAs were closely associated with tumor survival but no further experimental validation was carried out (85).

Therefore, Exosome-mediated communication plays an essential role in the hypoxic environment. Hypoxic exosome-shuttled bioactive non-coding RNAs have been shown as critical regulators of cancer proliferation.

2.2 Invasion and metastasis

Hypoxia has been demonstrated to regulate the invasion and migration ability of cancer cells mainly by promoting EMT. EMT is

involved in carcinogenesis and endows transformative properties to cancer cells by improving mobility, invasion, and migration (86). During EMT, downregulation of epithelial markers (E-cadherin and β-catenin) and upregulation of mesenchymal markers (N-cadherin and Vimentin) can occur, which then induce the mesenchymal phenotypes and enhance the metastatic ability of the cancer cells. Much attention has been drawn to exosomal non-coding RNAs in the hypoxic tumor microenvironment, given that they could govern metastatic and invasive capability of cancer cells by directly or indirectly targeting EMT markers. Li et al. reported that miR-21 increased in hypoxia-derived exosome promoted invasion and migration in oral squamous cell carcinoma (OSCC) by inducing EMT (72). In addition, lncRNA-UCA1 was present at a high level in the hypoxic exosomes from cancer cells than normoxic exosomes. The lncRNA-UCA1 secreted by hypoxic cancer cells promoted tumor progression through upregulating EMT in vivo and in vitro in bladder cancer (73). Exosomal miR-25-3p released from hypoxic breast cancer cells stimulated migration and proliferation of tumor cells by inducing IL-6 secretion and activating NF-κB signaling in macrophages. In vivo experiments revealed that injection of breast cancer cells with the miR-25-3p inhibitor substantially reduced the tumor size by inhibiting IL-6-mediated STAT3 activation (87).

Stromal cells are also indispensable components in the tumor microenvironment. Stromal-cancer or stromal-stromal interactions mediated by exosomes have profound impacts on metastasis initiation and cancer progression. Zhang et al. demonstrated that cancer cells could uptake exosomes derived from hypoxic bone marrow-derived mesenchymal stem cells (BMSCs) and acquire higher invasiveness. During this process, miR-193a-3p, miR-210-3p, and miR-5100 transferred into cancer cells and activated STAT3 signaling, thus inducing EMT in lung cancer cells. Furthermore, these three miRNAs were upregulated in the plasma-derived exosomes of patients than non-metastatic patients (88).

Metastatic colonization is profoundly affected by the hypoxic tumor microenvironment. Tumor-derived exosomes can reflect the hypoxic characteristics of the originating cell and also are capable of facilitating pre-metastatic niche formation by transmitting non-coding RNAs. Notably, organ-specific metastasis has gained much attention in recent years. Despite the hard work of many scientists, still little has been known about the mechanisms. Exploring exosomal non-coding RNAs could give rise to promising therapeutic targets as well as prognostic biomarkers of cancer metastasis.

2.3 Chemoresistance

Resistance to anti-cancer therapies is one of the biggest

obstacles in cancer treatment. Intrinsic resistance arises because of genetic alterations, whereas extrinsic resistance due to interactions between tumor cells and microenvironment against chemotherapy. Hypoxia affects the overall course of the tumor including responses to therapies. Hypoxia-induced malignancies could form resistance to various anti-cancer drugs including cisplatin, doxorubicin, sorafenib, etoposide, paclitaxel, and gemcitabine. (89). Also, researches have shown that anti-cancer drug resistance can be restored through inhibition of hypoxia-induced signaling pathway. Hypoxia could regulate chemoresistance of cancer cells by controlling cell cycle, autophagy, senescence of cells and chemotherapeutic efficacy through acidity as well as drug efflux pump expression. (90). Hypoxia-induced intracellular substances such as proteins and non-coding RNAs via exosomes secretion affect tumor microenvironment and cancer cell chemoresistance.

Dong et al. demonstrated that hypoxic non-small-cell lung cancer (NSCLC) cell-derived exosomes enhanced cisplatin resistance of normoxic cancer cells through transmitting miR-21. Mechanically, miR-21 in hypoxic exosomes downregulated phosphatase and tensin homolog (PTEN) and PI3K/ATK pathway sequentially, triggering cisplatin resistance in normoxic cancer cells. Further analysis with the TCGA database showed that miR-21

expression was positively correlated with HIF-1α and high miR-21 expression indicated worse survival in patients undergoing chemotherapy (91). Patel and his colleagues found linc-RoR, a stress-responsive lncRNA, regulated chemosensitivity of HCC cells to sorafenib, and doxorubicin. They described that linc-ROR expression was enhanced in the hypoxic cancer cell-derived exosomes. TGF-β enriched linc-RoR within exosomes, resulting in suppression of chemotherapy-induced cell death and tumor-initiating cell proliferation (92).

It is noteworthy that chemoresistance does not arise intrinsically in cancer cells. Many stromal cells like CAFs also support cancer cells to gain resistance to chemotherapy. MiR-223 was demonstrated to promote proliferation and invasiveness of ovarian cancer cells by targeting SOX11 expression (93) and it was the most significantly upregulated miRNA in the recurrent serous ovarian cancer tissues as compared to the primary tissues (94). On this basis, Zhu et al. observed the upsurge of miR-223 in TAMs and TAM-derived exosomes under hypoxia. MiR-223 conveyed by hypoxic exosomes could reduce apoptosis, increase cell viability and also increase drug resistance of ovarian cancer cells via downregulating PTEN expression and activating PI3K/AKT signaling pathway. Moreover, higher miR-223 expression was shown in the cisplatin-resistant

patients and recurrent patients in the epithelial ovarian cancer (EOC) patient-derived specimens. High expression of miR-223 together with low expression of PTEN indicated a bad prognosis of ovarian cancer patients (95).

These studies indicated chemoresistance could be passed through transmitting non-coding RNAs in exosomes in the hypoxic microenvironment. Blocking chemoresistance associated exosomal non-coding RNAs could be a promising way to overcome chemoresistance.

2.4 Immune suppression

In principle, tumor development can be monitored by cytotoxic innate and adaptive immune cells. However, as the tumor develops from dysplasia to clinically detectable tumors, cancer cells evolve different mechanisms such as losing expression of tumor antigens or modifying immune checkpoint molecules in order to avoid the destruction by the immune system (96). Tumor-derived exosomes have been shown to induce tumor-specific or nonspecific immune responses. Antigen-presenting cells could uptake tumor-associated antigens shuttled in exosomes and stimulate the tumor suppressive reactions (97). Hypoxic tumor exosomes have been demonstrated to suppress T cell proliferation and NK cell activation, induce macrophage M2 polarization and Regulatory T cells (Tregs)

activation, increase MDSC population resulting in immune dysfunction.

The interactions between tumor cells and T cells are critical in tumor immune microenvironment. Tumoral exosomes carrying biologically active non-coding RNAs transmit signals between cells, promoting tumor progression and immune escape. Ye et al. first reported that nasopharyngeal carcinoma (NPC) cell-derived exosomes impeded T cell dysfunction through differential miRNA expression (98). Building on this study, they further identified that tumoral exosomes could hamper T cell function by miR-24-3p delivery. Mechanistically, hypoxia-induced exosomal miR-24-3p inhibited T cell proliferation and Th1, Th17 differentiation and inducing T reg differentiation by targeting FGF11 followed by the upregulation of p-ERK, p-STAT1, p-STAT3 and downregulation of p-STAT5 (99).

T cell exhaustion is characterized as the upregulation of PD-1 on T cells. Blocking the PD-1/PD-L1 axis is the best way to reinvigorate T cell function (100). γδ T-cell is a unique lymphocyte population that has been reported to have either anti- or pro-tumoral functions. Li et al. revealed that normoxic OSCC-derived exosomes stimulated the γδ T-cell expansion and cytotoxic function in a dendritic cell (DC)-independent manner, which could be attenuated by miR-21 enriched hypoxic exosomes. MDSCs are a heterogeneous

immunosuppressive cell population from myeloid lineage migrating to the tumor site through circulation (101). A chronic inflammatory environment rich in cytokines like TNF, TGF-β and IL-10 triggers myeloid cells converting to MDSCs. Therefore, they are normally present in cancer or chronic inflammation associated diseases while not present in a steady state of healthy people (102). MDSCs suppress the adaptive and innate immunity through inhibiting T cell activation, promoting M2 polarization of macrophages, inducing CAF differentiation and inhibiting NK cell cytotoxicity, thus contributing to tumor angiogenesis, metastasis and drug resistance (103). The accumulation of MDSCs was shown to be correlated with poor clinical outcomes and reduce the efficacy of immunotherapy in cancer patients. Hence, eliminating and suppressing MDSCs is becoming a new therapeutic strategy (104). It was reported that exosome shuttled miR-21 secreted from γδ T cells could abate the function of MDSCs in a PD-L1-dependent manner through targeting PTEN(105). This study sheds new light on the effects of tumor-derived exosomes on the γδ T cells. Meanwhile, it also suggested that integrative inhibition of hypoxia-induced exosomal miRNAs and PD-1/PD-L1 axis would be a new insight in immunotherapy. In glioma, hypoxia-induced exosomal miR-21 and miR-10a presented the remarkable effects on the expansion and function of MDSCs in

vitro and in vivo via miR-21/PTEN/PI3K/AKT and miR-10a/RORA/IκBα/NF-κB axis respectively (106).

Hypoxia in the tumor microenvironment could stimulate immunosuppressive effects attenuating cytotoxic T-lymphocyte (CTL) and NK cell-mediated tumor cell lysis. Berchem et al. elucidated that lung cancer cells generated exosomes with higher miR-23a expression, which could impair NK cell cytotoxicity and NK cell function by directly targeting CD107a. Furthermore, higher TGF-β in the exosomes might partly contribute to the enrichment of miR-23a. This is the first study demonstrating how cancer cells in the hypoxic microenvironment educate NK cells through exosome transmitted non-coding RNAs (35).

Macrophages can be roughly classified into M1 (classically activated) macrophages with pro-inflammatory effects and M2 (alternatively activated) macrophages with anti-inflammatory effects. M1 macrophages characterized by the expression of the inducible type of nitric oxide synthase (iNOS) are proinflammatory, whereas M2 macrophages express high level of anti-inflammatory cytokines (e.g., IL10) and a potent arginase-1 (Arg1) activity to favor tumor cell growth (107). TAMs constitute a predominant population of immune-related stromal cells in the tumor microenvironment. TAMs were previously described as exhibiting M2-like function.

However, studies argue that TAMs can express hallmarks of both M1 and M2 polarization (108). Cancer cells under hypoxia pressure secreted more functional exosomes acted as a bridge between cancer cells and macrophages, especially inducing M2 polarization. Although M2 polarization is still the mainstream, altering TAMs to a predominantly M1 phenotype has been put on the agenda for developing new immunotherapeutic strategies. These results suggest that hypoxic exosomes are influential elements in the tumor microenvironment mediating the interactions between cancer cells and macrophages.

Hypoxic EOC cell-derived exosomes containing high levels of miR-940 stimulated the M2 polarization of macrophages. Then, miR-940-induced M2 macrophages, in turn, promoted EOC cell proliferation and migration. Interestingly, a high level of miR-940 was also observed in the malignant ascites-derived exosomes compared with benign peritoneal fluids (36). The same research team further explored the different miRNA expression profiling patterns between cancer cell-derived exosomes under hypoxia and normoxia. MiR-21-3p, miR-125 b-5p and miR-181 d-5p were selected as HIF-1α and HIF-2α induced miRNA candidates and then validated to affect macrophage M2 polarization through regulating SOCS4/5/STAT3 pathway (109). Moreover, exosomal miR-301a-3p

derived from hypoxic pancreatic cancer cells promoted macrophage M2 polarization through downregulation of PTEN expression and activating PI3Kγ signaling pathway, triggering the secretion of TGF-β, IL-10, and arginase from pancreatic cancer cells, which in turn, facilitated EMT and lung metastasis (110). Quantitative proteomics revealed that hypoxic mouse melanoma cell-derived exosomes were rich in immunomodulatory proteins and chemokines including CSF-1, CCL2, FTH, FTL, and TGFβ. Meanwhile, they detected that miRNA let7a was decreased in the hypoxic cells but dramatically increased in the released exosomes. Let7a-loaded exosomes enhanced mitochondrial oxidative phosphorylation system (OXPHOS) in macrophages through suppressing the insulin-AKT-mTOR signaling pathway (111).

Hypoxia pressure promoted the production and secretion of immune-modulating exosomes rich in non-coding RNAs. Exosome-mediated cancer-immune cell communication substantially impacts the immune reaction. Immune checkpoints are accessory molecules with T-cell activation or inhibition effects. Blockage of cytotoxic T-lymphocyte antigen 4 (CTLA-4) and PD-1 have heralded the dawn of an immune therapy era. Exosomal non-coding RNAs might be the indispensable targets for immune therapy based on their immune regulating functions.

2.5 Angiogenesis

Angiogenesis refers to a new blood vessel forming process and is an essential mediator for tumor progression. Hypoxia is one of the key factors in tumor angiogenesis. Vascular immaturity and weakened cell association of tumor blood vessel network can lead to excessive permeability, poor perfusion and increased hypoxia (112). Angiogenesis is a complicated process comprising of many genes, regulators, and pathways. VEGF is the crucial pro-angiogenetic growth factor stimulated by the alarm of hypoxia. Carmeliet et al. found that the hypoxic induction of VEGF decreased significantly in mouse embryonic stem cells by inhibiting HIF-1α (113). In addition to VEGF, HIF-1α is capable of regulating some other angiogenesis associated factors like platelet-derived growth factor (PDGF-B), vascular endothelial growth factor receptor-1(VEGFR-1), endothelin-1, iNOS and epidermal growth factor (EGF).

Recent studies have demonstrated that exosomal non-coding RNAs under hypoxic conditions could contribute to the angiogenesis process. For instance, miR-210 upregulated both in hypoxic leukemia cells and exosomes enhanced tube formation in endothelial cells (37).In NSCLC, HIF-1α induced microvascular miR-494 promoted angiogenesis both in vitro and in vivo through downregulating PTEN

and activating Akt/eNOS pathway (114). Another study in lung cancer showed that hypoxic exosomes promoted angiogenesis through transmitting miR-23a. Knockdown of HIF-1α prevented the increase of exosomal miR-23a while miR-23a inhibited HIF-1α regulators, PHD1 and PHD2 expression and enhanced HIF-1α signaling. Meanwhile, hypoxia-induced exosomal miR-23a could inhibit tight junction protein ZO-1 and increase vascular permeability (71). Interestingly, exosomal miR-23a upregulation was also observed in chemical-induced hypoxic liver cancer cell colonies established from culturing hepatic cancer cells on the soft agar. Results suggested that exosome-shuttled miR23a was capable of inducing angiogenesis by regulating pro-angiogenic marker genes and targeting SIRT-1 in chick chorioallantoic membrane (CAM), in ovo xenograft, and HUVEC model system (115). Umezu et al. established hypoxia-resistant multiple myeloma cell lines under 6 to 7 months hypoxic incubation to better mimic in vivo conditions of hypoxia bone marrow. Exosomal miR-135b derived from those cell lines enhanced endothelial tube formation under hypoxia via the HIF-FIH signaling pathway. Current studies mainly focused on acute hypoxia, which may differ from in vivo conditions. This is the first study that reported exosome-mediated cell-cell communication under chronic hypoxia (116).

Hypoxic exosomal non-coding RNAs can regulate angiogenesis by inducing phenotypic and functional changes in endothelial cells to promote tumor growth and metastasis. VEGFR inhibitors serve as the most vastly applied anti-angiogenesis agents now. They are bringing beneficial efficacies as well as nonnegligible problems like a double-edge sword. Exploiting the anti-angiogenesis potential of RNA therapy via exosomes might be a new therapeutic strategy in the future.

3. Clinical applications

Liquid biopsy is a new diagnostic tool performed on blood or other biofluids to assess the tumor-derived components and their genomic or proteomic profiles (117, 118). Circulating tumor cells (CTCs), circulating tumor DNAs (ctDNAs) are the primary analytes of liquid biopsies. However, recent studies have uncovered more liquid biopsy analytes including tumor-educated platelets, circulating non-coding RNAs, tumor-derived exosomes (119). Exosomes are released by almost all cell types and have been detected in various biofluids, including blood, urine, saliva, ascites, cerebrospinal fluids, etc. Exosomes and non-coding RNAs shuttled in exosomes have been demonstrated to play a vital role in cancer progression. Hypoxia is one of the critical characteristics in the microenvironment of most solid tumors. Analyzing exosomes or exosomal non-coding RNAs in the biofluids could monitor cancer progression, predict drug resistance, even detect tumor heterogeneity and trace tumor evolution, contributing to the precision therapy of cancer patients (Figure 3).

In vitro studies have shown that hypoxia could promote the production and release of exosomes of various cancer cell lines (67, 71, 115, 116). As a consequence, hypoxic tumors may increase the concentration of exosomes in the blood or other biofluids.

Daniela Ost et al. compared the concentration of plasma exosomes in patients with GBM and healthy controls where GBM patients showed significantly higher concentration. Intriguingly, the concentration decreased to an almost similar level to healthy controls after surgery while an increase was detected again at recurrence. This indicated that tumor cells mainly contributed to the exosome increment in plasma (120). Likewise, higher levels of exosomes were detected in the plasma of NPC patients than healthy controls and positively correlated with tumor lymph node metastasis and shorter disease-free survival (DFS)(98). These data suggested that circulating exosome enumeration is applicable to describe disease status and predict the clinical outcomes of patients.

However, the exosome releasing and producing processes are complicated and multifaceted. Hypoxia is not the sole factor influencing quantity and quality of exosomes. Besides, the mechanism of hypoxia in vivo might be quite different with that of in vitro models. Some other factors may also stimulate the release of exosomes including thermal stress, oxidative stress, tumor pH value, autophagy, endoplasmic reticulum stress, increase in intracellular Ca2+ levels or drug intervention (121). Therefore, circulating exosome quantification has many limitations due to its non-specificity. Analyzing exosome contents is needed to evaluate the

disease accurately.

Non-coding RNAs can be transferred through exosomes from tumor cells to adjacent cells or remote organs by entering the blood circulation. These non-coding RNAs are protected from degradation and stably exist in the circulation. Thus, exosomal non-coding RNAs derived from hypoxic tumors are detectable in the blood and might be used as biomarkers of cancer progression. Exosomes in the biofluids are a heterogeneous population of different cell origins. It is important to find tumor-specific non-coding RNA biomarkers. Recent studies have demonstrated different non-coding RNA profiles in the exosomes derived from cancer patients and healthy people through RNA-sequencing or RT-PCR analysis (53). Differently expressed non-coding RNAs generated from those studies could provide a large number of possible candidate biomarkers. By comparing exosomal non-coding RNA expression patterns at baseline, pre-treatment and post-treatment, correlating with clinical parameters, combining with continuous follow-up, it is possible to predict patient prognosis and therapeutic response. The combination of several non-coding RNA markers together may have favorable sensitivity and specificity than a single non-coding RNA. Wang et al. reported that the area under the ROC curve of dual detection of exosomal HOTAIR and miR-21 for diagnosing laryngeal squamous cell carcinoma reached 87.6 %,

significantly higher than 80.1 % of miR-21 or 72.7 % of HOTAIR (122). In addition, applying non-coding RNA biomarkers could compensate for the deficiency of clinical protein markers. For example, prostate-specific antigen (PSA) used for screening prostate cancer is of high sensitivity but low specificity in that it might also be upregulated in benign hyperplasia. The expression level of exosomal lncRNA SChLAP1 could help to differentiate prostate cancer and benign prostate hyperplasia patients when PSA was moderately elevated (123). Integrating in silicon analyses or in vitro experiments with the expression of non-coding RNAs in patient-derived samples is capable of selecting significant and functional non-coding RNAs of relative high specificity and sensitivity. In vitro models developed under hypoxic conditions can better mimic the in vivo state of the tumor microenvironment. Thus, hypoxia-induced exosomal non-coding RNAs might be of great significance in cancer diagnosis and monitoring.

Hypoxia-induced exosomal miR-23a and miR-24-3p were reported to be markedly higher in the serum of lung cancer patients and NPC patients, respectively, than that of healthy volunteers. Further analysis showed that the serum exosomal miR-24-3p level was negatively associated with the DFS of NPC patients (71, 99). Likewise, patients with OSCC had much greater expression of

circulating exosomal miR-21 compared with paired healthy donors. High circulating exosomal miR-21 levels were closely associated with the T stage and lymph node metastasis (72).Moreover, serum-derived exosomes of bladder cancer patients showed a significantly higher level of lncRNA UCA1 and, notably, the lncRNA UCA1 levels were positively correlated with HIF-1α expression. It could be speculated that intratumoral hypoxia might be capable of boosting exosome- shuttled lncRNA-UCA1expression. ROC analysis also showed fine specificity and sensitivity, suggesting its high diagnostic and clinical significance (73). In locally advanced rectal cancer (LARC), Tonje et al. filtered a series of exosomal miRNAs from five hypoxic cell lines and validated in patient plasma samples. Among these, downregulated miR-486-5p and miR-181a-5p were correlated with T4 and lymph node metastasis-positive disease, respectively, while upregulated exosomal miR-30d-5p was associated with the metastatic progression (124).

Hypoxia influences not only cancer cells but also stromal cells. Zhang et al. reported that hypoxic BMSC-derived exosomes could promote lung cancer metastasis through transmitting miR-193a-3p, miR-210-3p and miR-5100. Those three miRNAs expressed remarkably higher in the plasma-derived exosomes of lung cancer, liver cancer and pancreatic cancer patients than the counterparts of

healthy controls. In addition, ROC analysis of the individual miRNA or combination of three miRNAs panel all showed high specificity and sensitivity in distinguishing metastatic lung cancer patients and non-metastatic lung cancer patients (88).

Circulating exosomes can reflect the hypoxic feature of primary tumors. Therefore, non-coding RNAs loaded in circulating exosomes are emerging as new biomarkers of liquid biopsy in that they can dynamically mirror tumor burden or clinical events. As tumor progression and evolution is an intricate process, a single biomarker is far from comprehensively explaining the disease status. Integrative analysis of multiple biomarkers might be a prospective trend for clinical diagnosis. Although these researches have brought out new insights into the diagnostic and prognostic value of hypoxic tumor-derived exosomal non-coding RNAs, there are still some limitations. Studies discussed here had a minimal patient sample size so that large scale investigations are highly demanded to validate the clinical potential of hypoxic exosomal non-coding RNAs. Hypoxic exosomes can partially reflect the hypoxic feature of solid tumors. Researchers used different methods to induce hypoxia pressure which varied from oxygen concentration, hypoxic incubation time, etc. By far, there are no optimal in vitro systems to precisely mimic the in vivo hypoxic tumor microenvironment. Hypoxic exosome

concentration and cargo may fluctuate depending on different hypoxia generating means. Meanwhile, they were using different ways to isolate exosomes, which may cause nonnegligible variations as well. Thus, standardized protocols that can generate high purity of exosomes are undeniably needed for future clinical applications. Furthermore, recent researches preferred to use RNA sequencing or microarray to screen differently expressed non-coding RNAs, which could generate vast sets of candidate non-coding RNAs but at the same time increasing the difficulty of data analysis to a large extent. How to better analyze the data and related pathways also remains a big issue. Notably, which molecule to use to normalize the exosomal lncRNAs or miRNAs is still controversial.

Exosomes are stable, easy-stored, biocompatible, highly permeable, low toxic and immunogenic, which suffice almost all the merits of a good drug delivery system (125). Exosomes have the natural encapsulating ability to carry different anticancer drugs, natural agents, nucleic acid therapeutics including miRNAs, siRNAs or even gene-editing systems, such as CRISPR-Cas9 system. Notably, miRNAs and siRNAs transferred through exosomes to the recipient cells can partly or entirely abolish the expression of target genes, thus restricting tumor progression (125). The KRASG120 siRNA loaded in human-foreskin fibroblast-derived exosomes

efficiently suppressed pancreas desmoplasia in the orthotopic and genetically engineered mice (126). Despite the advantages over other drug delivery systems, exosomes are still facing unavoidable challenges. Exosome heterogeneity, unwanted immunogenetic possibility and the potential tumor promoting risks await resolutions before clinical translation (125).

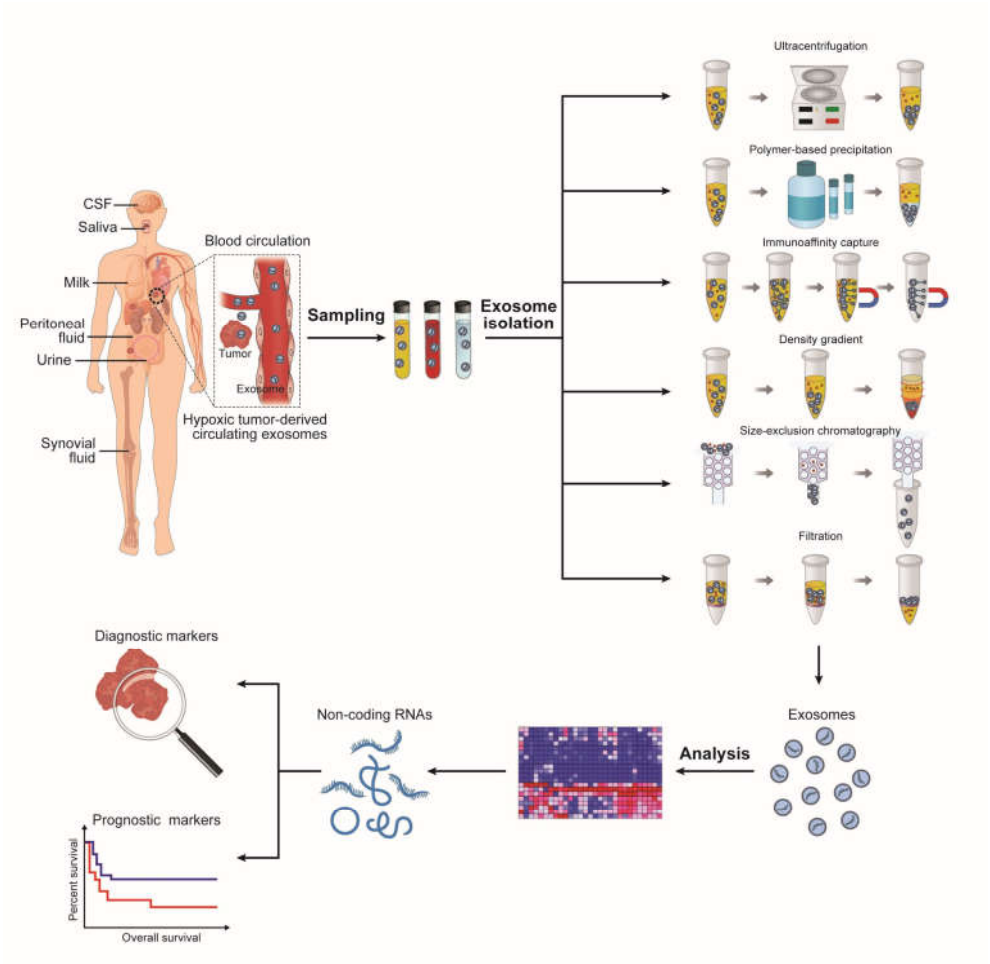
CSF
Saliva
Milk
Peritoneal fluid
Urine
Synovial fluid
Blood circulation
Tumor
Exosome
Hypoxic tumor-derived circulating exosomes
Sampling
Exosome isolation
Ultracentrifugation
Polymer-based precipitation
Immunoaffinity capture
Density gradient
Size-exclusion chromatography
Filtration
Exosomes
Analysis
Non-coding RNAs
Diagnostic markers
Prognostic markers
Percent survival
Overall survival

Figure 3. Hypoxic tumor-derived circulating exosomal non-coding RNAs in liquid biopsy

Exosomes are present in diverse biofluids including blood, cerebrospinal fluids, saliva, milk, peritoneal fluid, urine, synovial fluid, etc. Exosomes can be isolated from these biofluids and non-coding RNAs are then analyzed for diagnostic or prognosis markers. As illustrated on the right side of the figure, various methods have been developed to isolate exosomes with different advantages and disadvantages each (Ultracentrifugation: high sample capacity, minor impacts on exosomal components; time consuming, facility dependent. Polymer-based precipitation reagents: simple steps, possible for small sample volume, high yield; expensive reagents, low purity; Immunoaffinity capture: high purity and specificity; expensive reagent, low yield, antibody dependent; Density gradient separation: high purity; complicated procedures, low yield, facility dependent. Ultrafiltration: less time consuming; low purity and integrity).

Chapter 2.

Integrated analysis of ascites and plasma extracellular vesicles identifies a panel of miRNAs for ovarian cancer diagnosis

1. Introduction

Ovarian cancer is one of the leading causes of female cancer-related death worldwide (127, 128). Most ovarian cancer patients are typically diagnosed at advanced stages with a five-year survival rate less than 30%. Current screening tools such as the routine pelvic examination, transvaginal ultrasound, blood biomarker CA125 have been suffered from low sensitivity and specificity, especially in the early stages(129-131). It is an absolute necessity to identify reliable clinical biomarkers by non-invasive procedures for ovarian diagnosis.

Extracellular vesicles (EVs) are double-membrane nanoscale particles secreted by essentially all prokaryotic and eukaryotic cells into the extracellular space. EVs play a crucial role in mediating cell-to-cell interactions by transporting functional RNAs, proteins, lipids, etc. These EV cargos are stably encapsulated inside the double lipid layers devoid of nucleases, proteases or oxidase stress (32, 33, 132). EV RNA cargos include a wide range of RNA biotypes partially reflecting the RNA content of source cells, with a particular

preference for small non-coding RNAs. MicroRNAs (miRNAs) are a class of small non-coding RNAs comprising ~22 nucleotides in length. Ample evidence has depicted that miRNAs are actively involved in various biological processes by post-transcriptionally regulating gene expression. Recent studies have elucidated that the miRNA profiling of EVs is still significantly disparate from that of origin cells, suggesting the miRNA cargos are assembled in a selective manner. During the EV biogenesis process, miRNAs with high enrichment, the capacity of connecting to membranes, cytosolic subcellular location and specific RNA motifs possibly favor themselves encapsulated in EVs (133). Moreover, multiple lipids and RNA binding proteins are reported to regulate the RNA packaging to EVs, such as AGO2, ALIX, annexin A2, heterogeneous nuclear ribonucleoproteins A2/B1 (HNRNPA2B1), SYNCRIP, etc. (56, 58, 134-138). Additionally, different stimuli or treatments may also markedly impact the amounts and proportions of miRNA cargos. For example, hypoxia and acidosis can alter the quantity and composition of EV secretion (139, 140). EV miRNAs play a regulative role in cancer proliferation, invasion, migration, chemoresistance, angiogenesis, immune responses, reshaping the tumor microenvironment and serving as potential clinical biomarkers (132).

Liquid biopsy is emerging as a powerful approach for cancer

diagnosis and surveillance due to the minimal invasiveness and high accessibility. Circulating tumor cells (CTCs), circulating tumor DNAs (ctDNAs) are the most common sources in clinical settings while EVs have also been identified as essential analytes recently. EVs are detected in various biofluids including plasma, serum, urine, cerebrospinal fluid, saliva, ascites, etc. Emerging evidence has suggested that EVs may hold great potential as novel biomarkers for cancer liquid biopsy. Recent studies have depicted that EV miRNA signatures in the circulation are distinct between cancer types and can serve as potential clinical biomarkers.

Blood is the most widely used source for liquid biopsy with regard to its universality and high accessibility. However, the tumor-derived EV miRNA features might be highly diluted in the circulation. So it might be not easy to find highly cancer-specific biomarkers. Liquid biopsy is not limited to blood. Tumor-derived materials are released in many other fluids (urine, pleural fluids, cerebrospinal fluids, ascites etc.) in higher amounts when in direct contact with the primary tumors or metastatic sites [1]. Considering the disease feature of ovarian cancer, ascites enriched in ovarian tumor-derived substances including EVs would be a perfect source for identifying EV miRNA biomarkers reflecting ovarian tumor features. Therefore, exploiting ascites is fundamental for finding significant clinical

biomarkers. Meanwhile, blood is the most widely used source for liquid biopsy with regard to its universality and high accessibility. In this scenario, biomarkers discovered in the ascites that are simultaneously detectable in the blood will combine the merits of high efficacy and high accessibility. Herein, we conjointly investigated the miRNA profiling of ascites- and plasma-derived EVs to determine highly accurate and accessible biomarkers; and also explored the impact of ascites-derived EVs on the malignant phenotypes of ovarian cancer cells. This study underscores the fundamental role of EV miRNAs in ovarian cancer and sheds new light on the clinical translational potential of EV miRNAs-based liquid biopsy.

2. Materials and Methods

2.1. Clinical sample collection

This study was approved by the Institutional Review Board of Seoul National University Hospital (No. 2004-128-1117) and performed in accordance with the Declaration of Helsinki. All the ascites, peritoneal fluids, blood and tissues were collected with an acquisition of the written consent.

2.2. Ascites and plasma preparation

Ascites was collected and subsequently centrifuged at 2500 rpm, 4 ℃ for 10 minutes to separate the cellular fractions and acellular fractions. The acellular supernatant was filtered with a Falcon 70 μm strainer (Corning, USA), aliquoted and stored in -70 ℃ for future use. Whole blood was obtained in the EDTA-treated tubes and centrifuged at 2500 g, 4 ℃ for 15 minutes to remove cells. Then the supernatant was collected and centrifuged again to deplete the platelets. The centrifuged plasma was aliquoted and stored at -70 ℃ for future use.

2.3. EV isolation and identification

Ascites, plasma and cell culture media were thawed and filtered with a 0.2 μm syringe filter (Sartorius, Gottingen, Germany) before EV isolation. Commercial EV isolation kit ExoQuick (System Biosciences, USA) was used for ascites and plasma EV isolation

according to the manufacturer’s protocol.

2.4. Nanoparticle tracking analysis (NTA)

EV pellets were suspended in PBS and diluted to an appropriate concentration. EV concentrations and size distributions were measured by nanoparticle tracking analysis (NTA) with a NanoSight NS300 system (Malvern Technologies, Malvern, UK). Samples were introduced into the chamber using syringes and each sample was captured with three 30-second videos for further analysis.

2.5. Transmission electron microscopy (TEM)

EVs were suspended in PBS and 10 μL of each EV suspension was applied on a 200 mesh formvar-coated copper grid. Then the grid was negatively stained with 10 μL of 2% phosphotungstic acid. The imaging analysis was carried out using a JEM 1400 transmission electron microscope (Jeol Ltd, Peabody, USA).

2.6. Western blotting

The western blotting assay was performed as previously described (141). The following primary antibodies were used: CD9 (Santa Cruz, CA, USA), CD63 (Santa Cruz, CA, USA), CD81(Santa Cruz, CA, USA), ROR (Invitrogen, USA), GAPDH (Santa Cruz).

2.7. Small RNA sequencing

RNA was extracted and quantified using a NanoDrop 2000 Spectrophotometer system (Thermo Fisher Scientific, Waltham, MA,

USA). The library was constructed using NEBNext Multiplex Small RNA Library Prep kit New England BioLabs, Inc. USA according to the manufacturer's instructions. Briefly, for each sample, 1 μg of the total RNA was used to ligate adapters and cDNA synthesis was performed using the reverse transcriptase with adaptor-specific primers. PCR was carried out for library amplification and a clean-up was performed with the QIAquick PCR Purification Kit (Qiagen, Hilden, Germany) and AMPure XP beads (Beckmancoulter, CA, USA). The yield and size distribution of the small RNA libraries was determined by the Agilent 2100 Bioanalyzer instrument for the High sensitivity DNA Assay (Agilent Technologies, Santa Clara, CA, USA). Then the single-end 75 sequencing was performed of the high-throughput sequences generated by the NextSeq500 system (Illumina, SanDiego, CA, USA).

3. Results

3.1. Isolation and identification of EVs from ascites and plasma

Malignant ascites obtained from high-grade serous ovarian cancer (HGSOC) patients during surgery or abdominocentesis was processed into cellular fractions and acellular fractions for later use (Fig. 1A). Benign peritoneal fluids collected from female patients with benign gynecologic diseases were used as a control in this study. Similarly, malignant and benign plasma samples were also acquired from patients suffering from HGSOC or benign disorders. EVs were respectively isolated from benign peritoneal fluids (BA-EVs), malignant ascites (MA-EVs), benign plasma (BP-EVs) and malignant plasma (MP-EVs) with the commercial kit ExoQuick (Fig. 1B). The typical morphology of these EVs as nanosized double-membrane circular particles were identified by TEM (Fig. 1C). Western blotting demonstrated the positive expression of EV marker CD9 and CD81 (Fig. 1D). In addition, NTA assessed the size distribution of these EVs ranging from 30 nm to 200 nm (Fig. 1E). Steady and representative EV populations were generalized in this manner for further research.

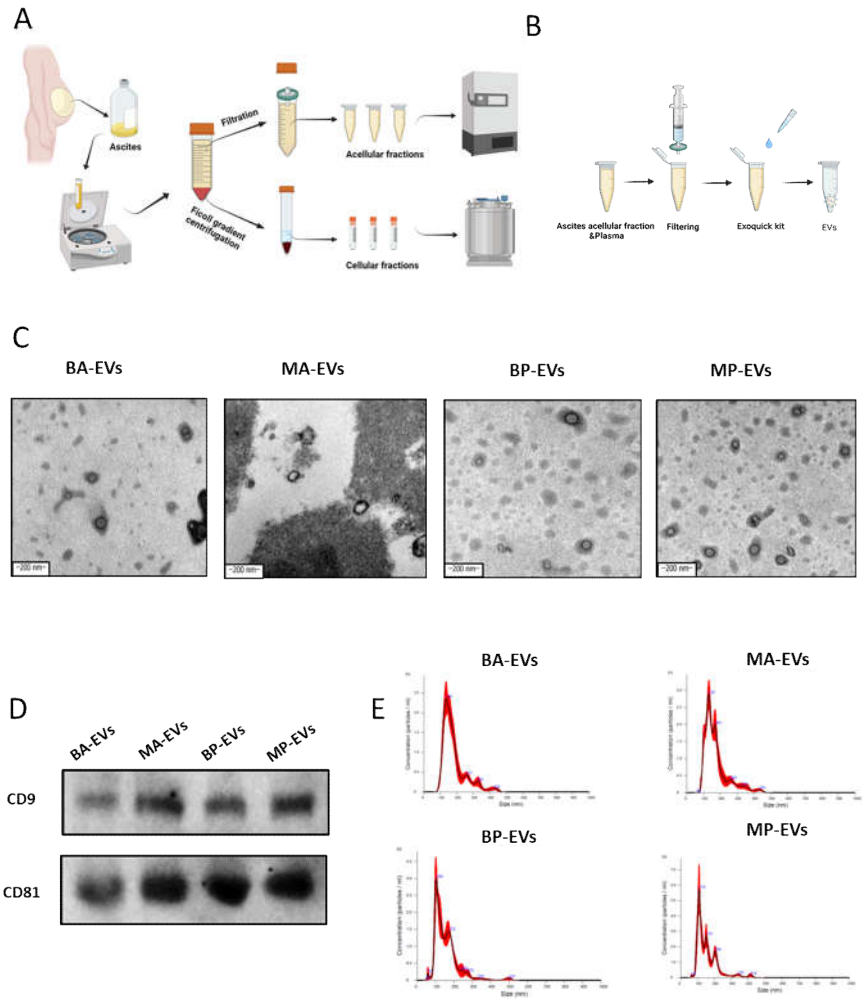
A
Ascites
Filtration
Ficoll gradient centrifugation
Acellular fractions
Cellular fractions
B
Ascites acellular fraction &Plasma
Filtering
Exoquick kit
EVs
C
BA-EVs
MA-EVs
BP-EVs
MP-EVs
D
BA-EVs
MA-EVs
BP-EVs
MP-EVs
CD9
CD81
E
BA-EVs
MA-EVs
BP-EVs
MP-EVs

Fig. 1. Isolation and identification of EVs from ascites and plasma.

A. The pipeline of ascites sampling. Malignant ascites obtained from HGSOC patients during surgery or celiac puncture were processed into cellular fractions and acellular fractions.

B. Isolation of EVs from ascites and plasma. Ascites acellular fractions and plasma were filtered and ExoQuick kit was applied for EV isolation.

C. TEM was performed to identify the morphology of BA-EVs, MA-EVs, BP-EVs and MP-EVs.

D. Western blotting was carried out to detect EV marker expressions of BA-EVs, MA-EVs, BP-EVs and MP-EVs.

E. NTA was used to identify size contribution and concentration of BA-EVs, MA-EVs, BP-EVs and MP-EVs. BA-EVs: benign peritoneal fluid-derived EVs; MA-EVs: malignant ascites-derived EVs; BP-EVs: benign plasma-derived EVs; MP-EVs: malignant plasma-derived EVs.

3.2. Ovarian cancer EV miRNA (OCEM) signature based on differentially expressed EV miRNAs between benign and malignant biofluids shows great performance in ovarian cancer diagnosis

Small RNA sequencing was carried out to investigate the miRNA profiling of MA-EVs (N=10) and BA-EVs (N=9) as well as MP-EVs (N=31) and BP-EVs (N=24). Differentially expressed miRNAs (DEmiRs) in ascites and plasma subset were relatively shown in Fig. 2A, B and Fig. 2C, D. The pathway analysis depicted that a large portion of DEmiRs was closely involved in carcinogenesis, cancer progression, multiple cancer hallmarks and EV genesis-related pathways (Fig. S1A, B & S2A, B). Next, to select candidate miRNAs for constructing the diagnostic signature, the in-house dataset was divided into the training and validation set (Fig. S3A); DEmiRs were analyzed in the training set only (Fig. S3B, C). According to the result, there were 17 DEmiRs overlapped in the ascites and plasma dataset (Fig. 2E). The univariate logistic regression analysis was carried out to decipher the diagnostic ability of each miRNA using the Area Under the Curve (AUC) of the receiver operating characteristic (ROC) curve. These 17 DEmiRs were ranked according to their AUC of detecting ovarian cancer patients in the ascites and plasma training set respectively (Fig. 2F, G). Eight miRNAs (miR-1246, miR-1290, miR-483-5p, miR-429, miR-34b-3p, miR-34c-5p, miR-

449a, miR-145-5p) that exhibited fine discrimination efficacy both in ascites and plasma were selected for the logistic regression analysis to construct the ovarian cancer EV miRNA (OCEM) signature (Fig. S3D). The expression of these eight miRNAs in the ascites and plasma subset was shown in the heatmaps (Fig.3H, I). The validation set of our in-house dataset was also applied to verify the performance of the OCEM signature. Results demonstrated that the OCEM signature yielded an excellent diagnostic ability both in ascites (Training set: AUC=1; Validation set: AUC=1) and plasma (Training set: AUC=0.9762; Validation set: AUC=0.9375) (Fig. 2J, L). The risk-probability plots showed OCEM signature could well differentiate benign peritoneal fluids and malignant ascites (Fig. 2K), as well as benign and malignant plasma (Fig. 2M). The detailed data illustrating the performance of OCEM signature was shown in Table 1.

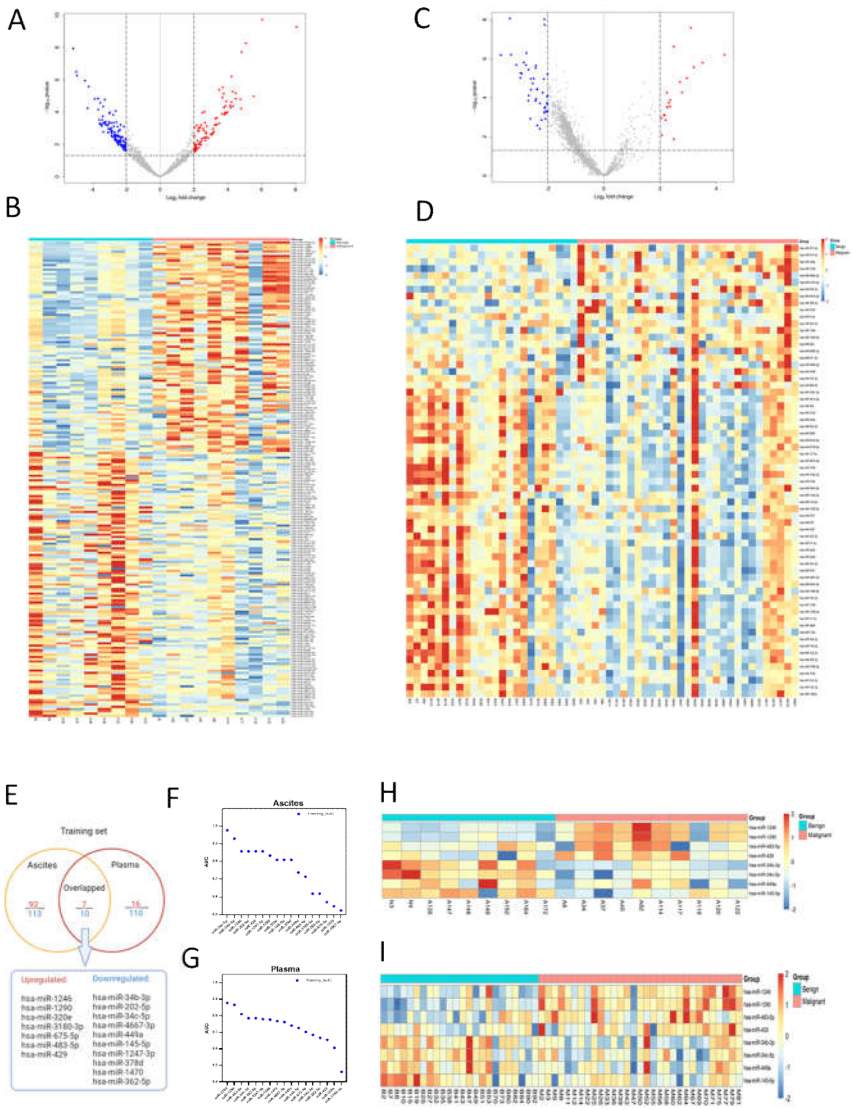
A
C
B
D
E
Training set
Ascites
Plasma
Overlapped
92
113
7
10
16
110
Upregulated:
hsa-miR-1246
hsa-miR-1290
hsa-miR-320e
hsa-miR-3160-3p
hsa-miR-675-5p
hsa-miR-483-5p
hsa-miR-429
Downregulated:
hsa-miR-34b-3p
hsa-miR-202-5p
hsa-miR-34c-5p
hsa-miR-4667-3p
hsa-miR-449a
hsa-miR-145-5p
hsa-miR-1247-3p
hsa-miR-378d
hsa-miR-1470
hsa-miR-362-5p
F
Ascites
G
Plasma
H
I
J
Ascites
K
Training set
Validation set
Cancer
Non-Cancer
Risk Probability
L
Plasma
M
Training set
Validation set

Fig.2. OCEM signature construction based on miRNA expression profiling of biofluids-derived EVs.

Small RNA sequencing was carried out to investigate the miRNA profiling of MA-EVs (N=10) and BA-EVs (N=9) as well as MP-EVs (N=31) and BP-EVs (N=24). MiRNAs with the expression altered at least 4 folds with a P value<0.05 between benign and malignant groups were regarded as differentially expressed miRNAs (DEmiRs).

A. The volcano plot showed DEmiRs in the ascites subset (Upregulated: N=93; Downregulated: N=117).

B. The heatmap illustrated the expression pattern of DEmiRs in the ascites subset.

C. The volcano plot demonstrated DEmiRs in the plasma subset (Upregulated: N=21; Downregulated: N=45).

D. The heatmap showed the expression pattern of DEmiRs in the plasma subset.

E. The Venn diagram depicted that 17 were DEmiRs overlapped (Upregulated: N=7; Downregulated: N=10) in the ascites and plasma training set.

F. The univariate logistic regression analysis demonstrated the AUC of these 17 DEmiRs in identifying cancer patients in the ascites training set.

G. The univariate logistic regression analysis demonstrated the AUC of these 17 DEmiRs in detecting cancer patients in the plasma training set.

H. The heatmap showed the expression of 8 miRNAs selected for constructing the OCEM signature in the ascites subset.

I. The heatmap illustrated the expression of 8 miRNAs selected for developing the OCEM signature in the plasma subset.

J. ROC curves elucidated the diagnostic ability of the OCEM signature in the ascites training and validation set.

K. ROC curves showed the diagnostic performance of the OCEM signature in the plasma training and validation set.

L. The risk-probability plots demonstrated the predictive risk probabilities in the ascites training and validation set.

M. The risk-probability plots showed the predictive risk probabilities in the plasma training and validation set.

A

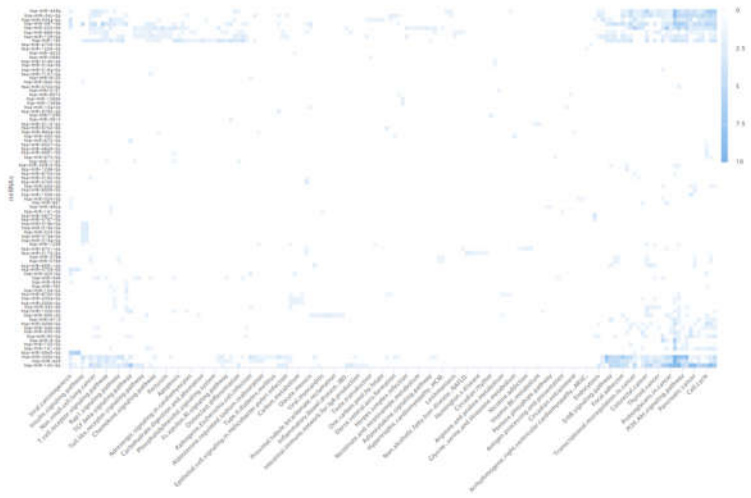

B

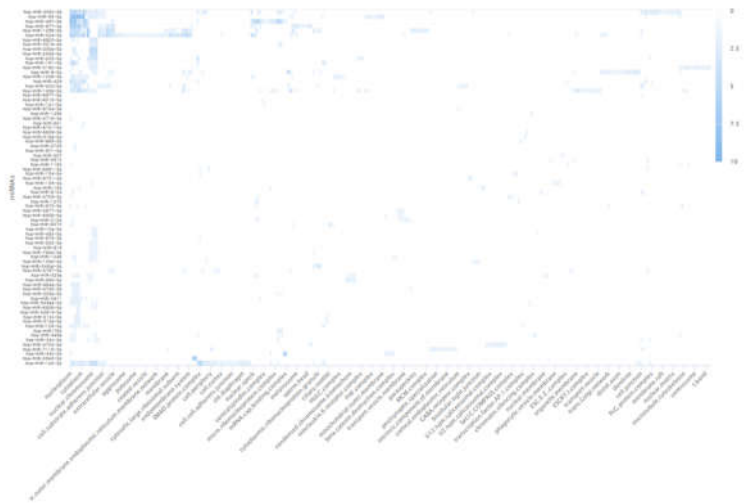

Fig. S1. A. The KEGG pathway analysis of DEmiRs in the ascites subset. B. The Gene Oncology (Cellular Components) analysis of DEmiRs in the ascites subset.

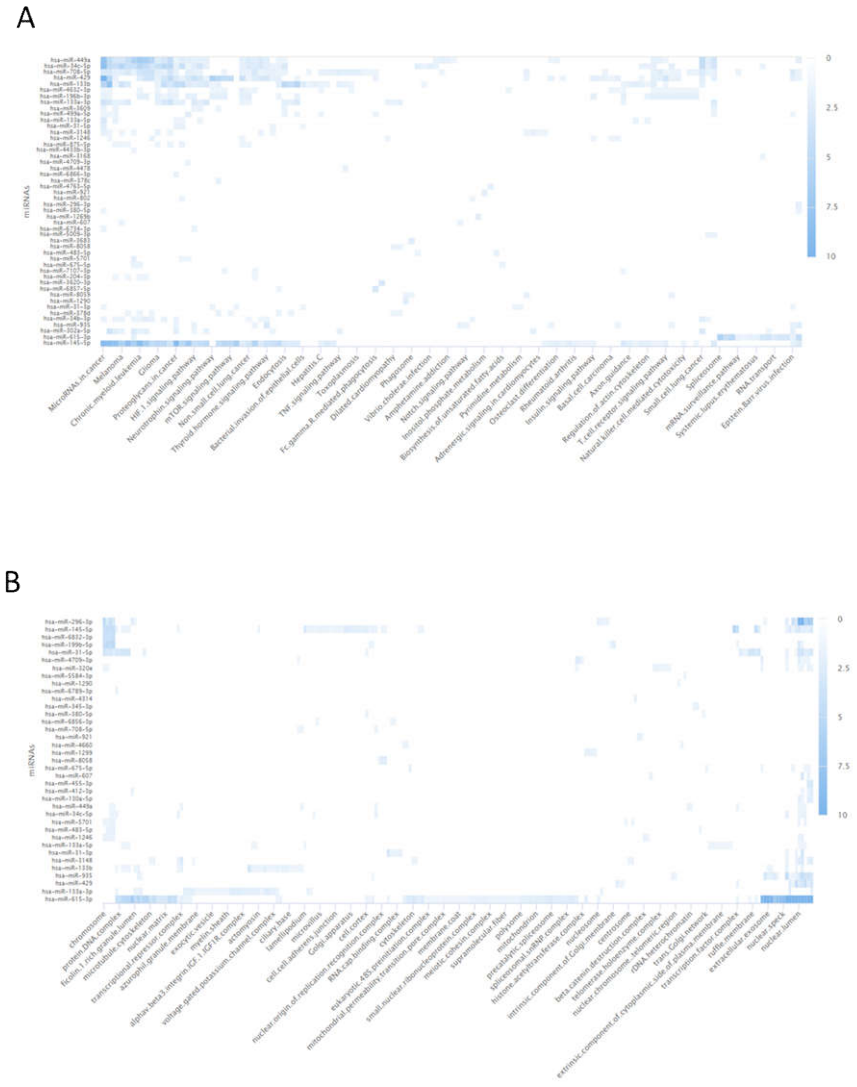

Fig. S2. A. The KEGG pathway analysis of DEmiRs in the plasma subset. B. The Gene Oncology (Cellular Components) analysis of DEmiRs in the plasma subset.

A

Sample	Training		Validation		Total
	B	M	B	M	
Ascites	6	7	3	3	19
Plasma	16	21	8	10	55

B

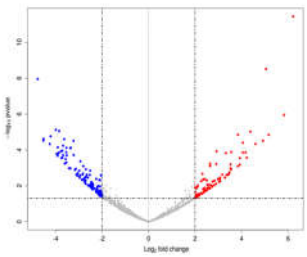

C

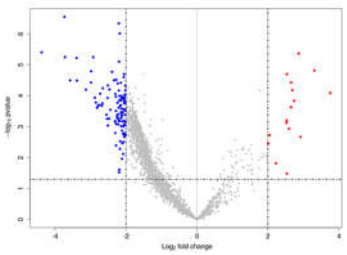

D

No.	miRNA	Expression in M
1	hsa-miR-1246	Upregulated
2	hsa-miR-1290	Upregulated
3	hsa-miR-483-5p	Upregulated
4	hsa-miR-429	Upregulated
5	hsa-miR-34b-3p	Downregulated
6	hsa-miR-34c-5p	Downregulated
7	hsa-miR-449a	Downregulated
8	hsa-miR-145-5p	Downregulated

Fig. S3. A. The in-house dataset was divided in to training set and validation set. B. The volcano plots showed that DEmiRs (Upregulated: N=92; Downregulated: N=113) in the ascites training set. C. The volcano plots showed that DEmiRs (Upregulated: N=16; Downregulated: N=110) in the plasma training set. D. Eight miRNAs selected for OCEM signature construction were summarized in the table.

Table 1. The performance of the OCEM signature in our in-house dataset and public datasets.

Dataset	Training set					Validation set				
	Accuracy	Balanced Accuracy	Sensitivity	Specificity	AUC	Accuracy	Balanced Accuracy	Sensitivity	Specificity	AUC
SNUH-Ascites	1.00	1.00	1.00	1.00	1.00	1.00	1.00	1.00	1.00	1.00
SNUH-Plasma	1.00	1.00	1.00	1.00	1.00	0.83	0.81	1.00	0.63	0.94
GSE106817	0.89	0.90	0.91	0.88	0.96	0.87	0.89	0.91	0.87	0.95
GSE83693	1.00	1.00	1.00	1.00	1.00	0.90	0.75	1.00	0.50	1.00
GSE65819	1.00	1.00	1.00	1.00	1.00	1.00	1.00	1.00	1.00	1.00
GSE113486	0.81	0.81	0.80	0.82	0.90	0.83	0.78	0.65	0.90	0.91
GSE58517	1.00	1.00	1.00	1.00	1.00	0.83	0.83	1.00	0.67	1.00
E-MTAB-4667	0.87	0.89	0.86	0.92	0.96	0.87	0.83	0.90	0.75	0.90
GSE127873	1.00	1.00	1.00	1.00	1.00	0.94	0.90	1.00	0.80	0.91

3.3. Logistic models based on OCEM signature exhibit excellent diagnostic performance irrespective of the clinical sample type (blood, tissue and urine) in different populations from multiple public datasets

Multiple public datasets were utilized to validate the robustness of the OCEM signature. Considering the heterogeneity in miRNA detecting platforms and batch effect between datasets, we retrained the OCEM signature independently in each dataset. We first applied serum dataset GSE106817 (Cancer: N=333; Non-cancer: N=2788) and GSE113486 (Cancer: N=40; Non-cancer: N=100) for validation. The OCEM signature showed great discriminative performance in detecting ovarian cancer patients of all stages in GSE106817 (Training set: AUC=0.9557; Validation set: AUC=0.9515) (Fig. 3A) and GSE113486 (Training set: AUC=0.904; Validation set: AUC =0.905) (Fig.3C). The risk-probability plots demonstrated that the OCEM signature well distinguished cancer and non-cancer individuals (Fig. 3B, D).

Subsequently, we validated the OCEM signature in the tissue miRNA profiling dataset GSE83693 (Cancer: N=80; Non-cancer: N=7) and GSE65819 (Cancer: N=16; Non-cancer: N=4) based on the hypothesis that the EV miRNA signature detected in the ascites and plasma could also reflect the characteristics of cancer tissues. Both

the OCEM signature displayed excellent diagnostic capacity in GSE83693 (Training set: AUC=1; Validation set: AUC =1) (Figure 3E) and GSE65819 (Training set: AUC=1; Validation set: AUC =1) (Figure 3G). The risk-probability plots elucidated that OCEM signature could almost perfectly differentiate cancer and normal tissues (Fig 3F, H). Intriguingly, the OCEM signature was also applicable in urine dataset GSE58517 (Cancer: N=80; Non-cancer: N=7) with a robust diagnostic ability (Training set: AUC=1; Validation set: AUC =1) (Figure 3I, J). Besides, some datasets only including seven or six miRNAs could also yield a high AUC in diagnosing ovarian cancer including stage I patients (Fig. S4A, B, C, D). These results highlighted the clinical applicability of the OCEM signature in diverse patient populations across multiple sample types.

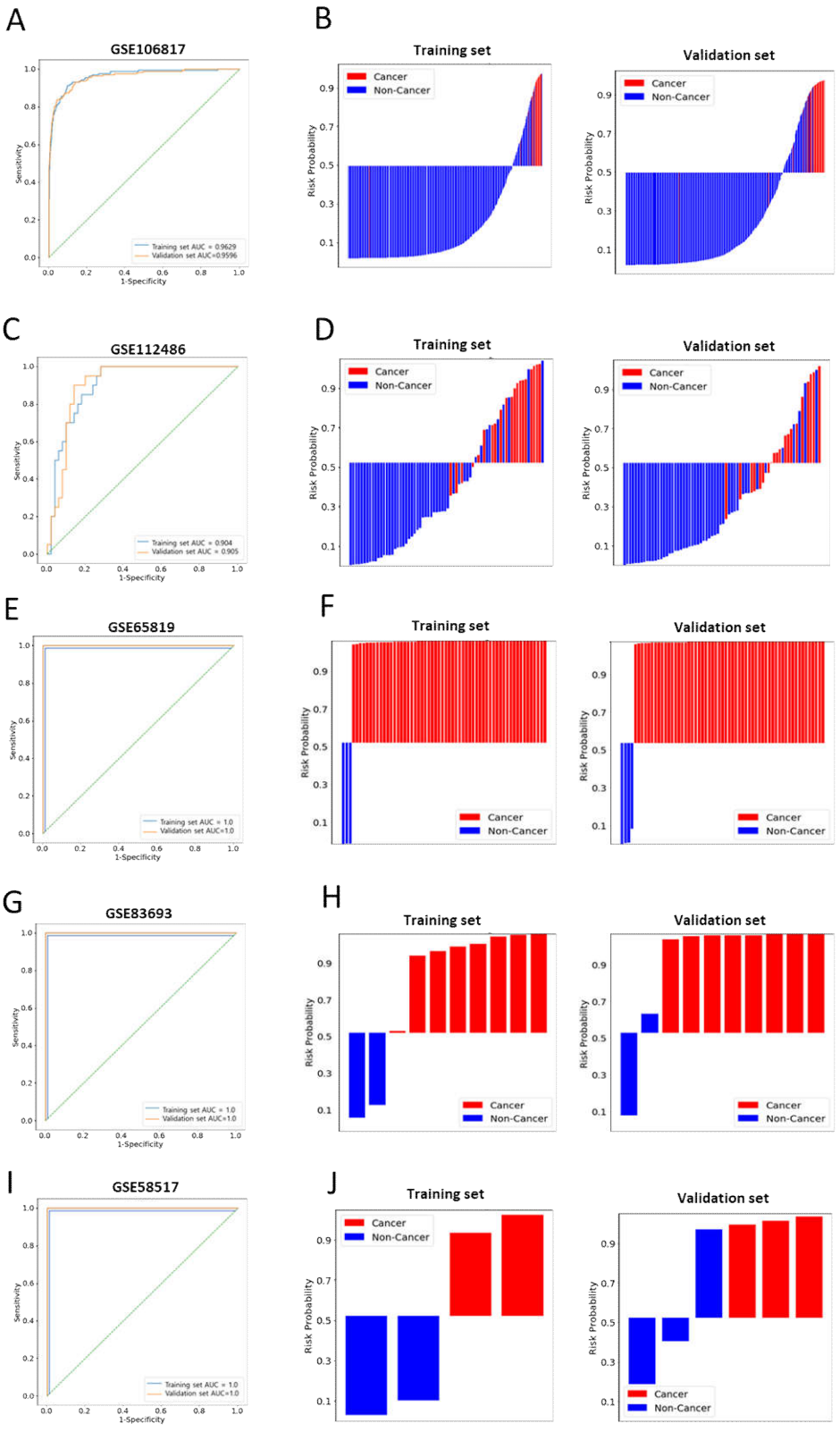
A
GSE106817
Sensitivity
1-Specificity
Training set AUC = 0.9629
Validation set AUC=0.9596
B
Training set
Validation set
Cancer
Non-Cancer
Risk Probability
C
GSE112486
Training set AUC = 0.904
Validation set AUC = 0.905
D
E
GSE65819
Training set AUC = 1.0
Validation set AUC=1.0
F
G
GSE83693
H
I
GSE58517
J

Fig.3. Validation of OCEM signature using diverse public datasets across multiple sample types.

ROC curves and risk-probability plots of the OCEM signature in

A, B. Serum dataset GSE106817 (Cancer: N=333; Non-cancer: N=2788).

C, D. Serum dataset GSE113486 (Cancer: N=40; Non-cancer: N=100).

E, F. Tissue dataset GSE83693 (Cancer: N=80; Non-cancer: N=7).

G, H. GSE65819 (Cancer: N=16; Non-cancer: N=4). I, J. Urine dataset GSE58517 (Cancer: N=80; Non-cancer: N=7).

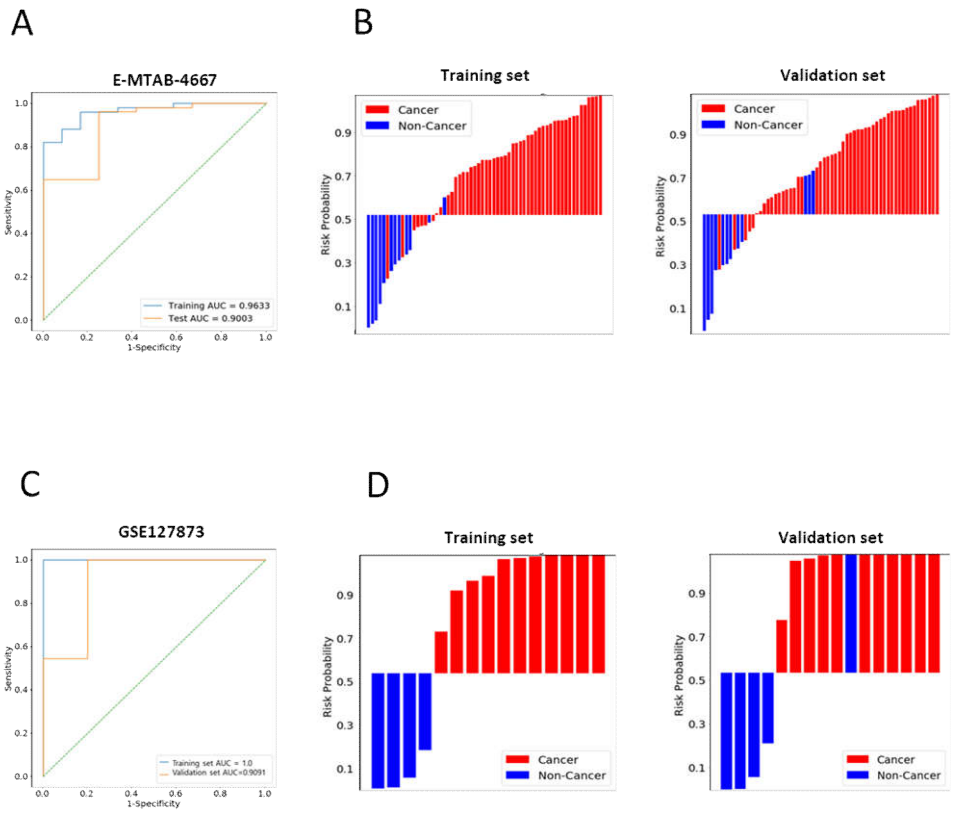

Fig. S4. ROC curves (A) and risk-probability plots (B) of 7 miRNAs (miR-1246, miR-1290, miR-483-5p, miR-34b-3p, miR-34c-5p, miR-449a, miR-145-5p) out of the OCEM signature in serum dataset E-MTAB-4667 (Cancer: N=106; Non-cancer: N=24). ROC curves (C) and risk-probability plots (D) of 6 miRNAs (miR-483-5p, miR-429, miR-34b-3p, miR-34c-5p, miR-449a, miR-145-5p) out of the OCEM signature in tissue dataset GSE127873 (Stage I cancer: N=22; Non-cancer: N=9).

4. Discussion

Multiple cellular and acellular components in the malignant ascites forms a perfect ecosystem for ovarian cancer progression. Malignant ascites in close contact with the tumor may contain more abundant tumor-derived substances, serving as a superior source to explore ovarian cancer-related EV biomarkers. However, there are also some restrictions hindering using ascites for the liquid biopsy on some occasions on account that ascites is not present in all patients and the abdominocentesis is still mildly invasive. Blood is the most widely used source for liquid biopsy owing to its high accessibility, non-invasiveness whereas tumor-derived EV signatures might be fairly diluted in the circulation. Biomarkers discovered in the ascites that are simultaneously detectable in the blood will combine the merits of high efficacy and high accessibility. In this scenario, we isolated the EVs from malignant ascites and plasma as well as the benign counterparts to explore candidate miRNA biomarkers. Optimized protocols were applied in this process including the sample collection, handling, storage, EV isolation and miRNA sequencing. We developed the OCEM signature with eight DEmiRs overlapped in the ascites and plasma subset, which showed an excellent discriminative performance in detecting HGSOC patients in our in-house dataset. miR-1246, miR-1290, miR-145 and miR-34b-

3p in the OCEM signature were also reported as potential diagnostic biomarkers in ascites or plasma in previous studies (142-146). It is noteworthy that we independently validated the diagnostic signature in public datasets and demonstrated that the OCEM signature showed a robust diagnostic ability across heterogeneous patient populations, various histologic characteristics, different stages and multiple sample types. Our results strongly suggest the superiority and clinical translational potential of the OCEM signature. On the other hand, there are some regrets in our study. First, the sample size of the in-house dataset was limited resulting from the sample rarity and strict quality control criteria. Second, ascites and plasma samples were not obtained from sample patients, which hindered the combined analysis of EV miRNAs in the ascites and blood. Third, our study is a cross-sectional study and a longitudinal observation is warranted in the further study. Before the implementation of OCEM signature in the clinical settings, a series of stringent criteria must be taken into consideration. Most importantly, the standardized protocols for biofluid sample collection, EV isolation, miRNA profiling, data analysis, etc. are undoubtedly required for yielding reliable and reproducible results. Also, more large-scale and long-term investigations are necessary to validate the efficacy of the identified biomarkers.

Representative EVs and EV cargos including miRNAs can be successfully detected in the ascites and plasma, suggesting these EVs could reflect the biological status and behaviors of tumors inside the body. Substantial progress has been made recently in addressing the clinical translational potential of EV-derived biomarkers in liquid biopsy. However, there are still many technological and scientific issues remained to be solved. EV heterogeneity is one of the major obstacles that has to be addressed by the following researches. EV populations in the biofluids are multi-originated and heterogeneous in size, composition and function, posing significant challenges in their characterization and applications. It is of great importance to identify reliable markers for EVs of different origins and seperately isolate EV subpopulations in the future. Besides, EV cargos including miRNAs are secreted in a selective manner from parental cells; more in-depth studies are warranted for demonstrating the underlying mechanisms. Moreover, as EVs are carriers of various biological signaling molecules, comprehensive multi-omics analysis of EV cargos is increasely crucial in improving the clinical validity and utility of EV-based liquid biopsy.

Chapter 3.

Malignant ascites-derived EVs facilitate the invasion and migration of ovarian cancer cells through transferring miR-1246 and miR-1290

1. Introduction

Hypoxia is a common feature in the microenvironment of most solid tumors (9). Clinical studies have revealed that overexpression of hypoxia-induced genes is associated with poor prognosis in many cancer types including pancreatic, lung, breast, prostate and ovarian cancer (10-14). Besides, plentiful in vitro and in vivo experimental data have suggested that hypoxia orchestrates malignant phenotypes of cancer cells through activation of multiple oncogenic signaling pathways. Transcription factors and epigenetic regulators can concertedly exert reinforcement of oncogenic signaling pathways, controlling the expression of numerous genes under hypoxia. Nevertheless, interactions between cancerous cells and non-cancerous cells could be further invigorated in the hypoxic tumor microenvironment. Cancer cells stimulated by hypoxia manifest increased drug-resistance, tumorigenesis, angiogenesis, invasiveness and immune suppression (15).

EVs are secreted by almost all the cells and molecular cargos of

EVs can partially reflect the characteristics of originating cells. EV-mediated cell-to-cell interactions in the microenvironment are critical in cancer progression. Recent studies have shed light on the EV miRNA expression and function shift in the hypoxic tumor microenvironment. Especially with the development of sequencing technology, more and more significant miRNAs are being uncovered. It has been reported that miR-21, miR-23a, lncRNA-UCA1 were upregulated in the exosomes derived from hypoxic cancer cells and promoted cancer progression in various signaling pathways (71-73). Hypoxia could induce the expression of circDENND2A, which could promote the migration and invasion of glioma cells through sponging miR-625-5p (75).

Ovarian cancer is one of the leading causes of female cancer-related death worldwide (127, 128). Most ovarian cancer patients are typically diagnosed at advanced stages with a five-year survival rate less than 30%. In ovarian cancer, the transcoelomic route is the most common and earliest route of metastasis, characterized by peritoneal dissemination and formation of malignant ascites (147). Malignant ascites is detected in over one-third of ovarian cancer patients and present in almost all the patients suffering from recurrence. Malignant ascites acts as a reservoir comprised of multiple cellular components and soluble factors, forming a characteristic tumor

microenvironment in ovarian cancer (148) (149). Exploiting ascites is fundamental to understanding the pathophysiology of peritoneal metastasis. In this study, we aimed to investigate the impact of ascites-derived EVs on ovarian cancer malignant phenotypes.

Our previous study has demonstrated eight miRNAs in the OCEM signature, among which, four were upregulated and four were downregulated in the malignant ascites-derived EVs than the benign ones. miR-1246 and miR-1290 were the most upregulated miRNAs and the absolute expression levels of these two miRNAs were remarkably high. We hypothesized that hypoxia might be a potential factor inducing the miRNA expression alteration and carried out experiments to validate our hypothesis. In addition, we also explored the function of miR-1246 and miR-1290 in regulating the aggressive behaviors of ovarian cancer cells.

2. Materials and Methods

2.1. Cell culture

Human ovarian cancer cell lines SKOV3 and KURAMOCHI used in this study were obtained from the American Type Culture Collection (Rockville, MD). Cells were cultured in RPMI1640 (WelGENE, Seoul, Korea) supplemented with 10% fetal bovine serum (FBS; Gibco, MD, USA) and 100 μg/mL penicillin-streptomycin

(Invitrogen, Carlsbard, CA, USA) in 37 ℃, 5% CO_2.

2.2. EV labeling and uptake

Isolated EVs were labeled with PKH67 green fluorescent cell linker mini kit (Sigma, USA) and cell membranes were labeled with PKH26 red fluorescent cell linker mini kit (Sigma, USA) according to the manufacturer's instructions. Labeled ovarian cancer cells were co-cultured with labelled EVs for 6 hours. The uptake of EVs by ovarian cancers was detected using the confocal microscopy LSM800 (EVOS, USA).

2.3. Invasion and migration assay

Transwell inserts with an 8 μm pore size (BD Biosciences, CA, USA) were used to investigate the invasion and migration potential of ovarian cancer cells. For invasion assay, inserts were pre-coated with the Matrigel (BD Biosciences, CA, USA). Briefly, ovarian cancer cells were seeded in the upper chamber in serum-free media and starved for 24 hours. Then the conditioned media with 10% FBS was added to the lower chamber. Cells were washed and stained with 0.5% crystal violet after 24 hours. Then cells that remained on the upper surface of inserts were removed while cells passing through the membrane were captured under a microscope and further analyzed by Image J software.

2.4. Organoid establishment

Malignant ascites-derived cells were used for establishing ovarian cancer organoids. Cells were embedded in phenol red-free Matrigel Growth Factor Reduced Basement Membrane Matrix (BD Bioscience, CA, USA) and cultured in organoid culture media. The organoid culture media was constituted of advanced DMEM/F12 (Gibco, MD, USA) supplemented with Penicillin/Streptomycin (Gibco), HEPES (Gibco), GlutaMax (Gibco), b-Estradiol (Sigma), Nicotinamide (Sigma), recombinant human Noggin (Peprotech), recombinant R-Spondin1 (RSPO1; Peprotech); B27 (Invitrogen), EGF (Invitrogen), FGF10 (Peprotech), HeregulinB-1 (Peprotech), Forskolin (bio-techne), Hydrocortisone (Sigma), A83-01 (bio-techne), Y-27632 dihydrochloride (Sigma), N-acetylcysteine (Sigma), Primocin (InvivoGen).

2.5. 3D invasion assay

Primary cancer cells (A37) from malignant ascites were used for tumor spheroid formation and 3D invasion assay. Cells were seeded in the Ultra-Low Attachment 96 well-plate (Corning, USA) to form spheroids. Three days later, EVs were added with Matrigel to the 3-day old spheroids for the 3D invasion assay. Images were taken after 72 hours and analyzed using ImageJ.

2.6. RNA extraction and quantitative real-time PCR

RNA was extracted from EVs using the RNA extraction kit

(Qiagen, Hilden, Germany) and transcribed into cDNA using miRCURY LNA RT kit (Qiagen, Hilden, Germany) with spike-in control Unisp6 added according to the manufacturer's instructions. Quantitative real-time PCR was performed using a miR-X™ miRNA qRT-PCR TB Green® Kit (Takara, Tokyo, Japan).

2.7. Transfection

miRNA mimics or inhibitors were transfected using Lipofectamine RNA iMAX (Invitrogen, Carlsbad, CA, USA) while plasmids were transfected using Lipofectamine 3000™ reagent (Invitrogen, Carlsbad, CA, USA). Culture media was changed six hours post-transfection. Cells were harvested for further analysis after incubation in complete culture media for 24 hours or 48 hours.

2.8. Ex vivo migration assay

The ovarian cancer patient-derived omentum adipose tissue was used to develop the ex vivo model. SKOV3^{luc} cells (luminescent SKOV3 cells) were transfected with different miRNA inhibitors or mimics and seeded in the ultra-low attachment 6-well plate (Costar, Corning, NY, USA) 24h post transfection. Ovarian cancer patient-derived omentum adipose tissues were cut into small pieces in same weight (75mg) and co-cultured with SKOV3^{luc} cells. After five days, the tissue pieces were transferred in a new plate and the number of SKOV3^{luc} cells having migrated to the omentum tissue pieces was

determined by the luminescence intensity measured with IVIS 100 imaging system (Xenogen, Alameda, CA, USA).

2.9. Luciferase reporter assay

Cells are co-transfected with pGL-3-RORα 3' UTR reporter plasmid (Origene, Rockvile, USA) containing the wild or mutated type miR-1246 or miR-1290 binding sequence and together with miR-1246 or miR-1290 mimics (Bioneer, Seoul, Korea) or negative control using Lipofectamine3000 (Invitrogen, USA). Luciferase Reporter Gene Detection Kit (MilliporeSigma, Missouri, USA) was used to detect the Firefly luciferase. The Firefly luciferase activity was calculated relative to the red fluorescence protein (RFP) intensity.

2.10. Immunohistochemistry (IHC)

The IHC assay was carried out using the 4μm thick tissue microarray (TMA) sections with a Benchmark autostainer (Ventana, Tucson, AZ, USA) according to the manufacturer's instructions as previously described (150).

2.11. Statistical analysis

Data were presented as mean ± SEM using GraphPad Prism 9. Statistical comparisons were performed using Student's t-test and one-way ANOVA analysis with Bonferroni's post hoc test. All the statistical analysis was two-sided with a p-value <0.05 considered

statistically significant.

3. Results

3.1. Malignant ascites-derived EVs facilitate the aggressive property of ovarian cancer cells in 2D and 3D culture models

Previous reports have demonstrated that circulating EV concentrations were informative in cancer diagnosis and cancer progression monitoring (120). However, few studies have reported the clinical significance of EV concentration in ascites. We compared the EV concentration between benign peritoneal fluids and malignant ascites using NTA. The result showed that EV concentration was significantly increased in malignant ascites compared to benign peritoneal fluids (Fig. 1A). In addition, we observed an elevated level of EV concentration in advanced-stage (stage III and IV) cancer patients than in early-stage (stage I+II) ones (Fig. 1B). It has been previously demonstrated that anti-cancer treatment could have an impact on EV secretion in cancer patients (120, 151, 152). Our result also depicted that recurrent cases had a more enriched EV level in the ascites compared to patients at primary diagnosis (Fig. 1C). These data suggested that MA-EVs concentration may be significantly instructive in monitoring cancer progression.

It has been demonstrated that malignant ascites forms a

supportive microenvironment for peritoneal dissemination. To investigate the effect of MA-EVs on ovarian cancer malignant phenotypes, we treated these EVs to ovarian cancer cell lines SKOV3 and KURAMOCHI. The uptake of MA-EVs by cancer cells was shown in Fig. 1D. Noticeably, MA-EV treatment significantly promoted the invasion and migration of SKOV3 and KURAMOCHI cells while BA-EVs showed no significant effect (Fig. 1E). Detached ovarian cancer cells floating in ascites usually colonize to metastatic sites either in single cells or multicellular spheroids. Therefore, we carried out a 3D spheroid invasion assay mimicking tumor micro-metastasis to further explore the impact of MA-EVs on tumor spheroids. The result showed that spheroids treated with MA-EVs exhibited increasing invasive ability than those treated with BA-EVs or PBS (Fig. 1F). Human organoids have emerged as an extraordinary model bridging the gap between in vitro and in vivo preclinical cancer models (153). We developed the ascites cell-derived organoids and tested the effect of MA-EVs in this in vivo-like in vitro model. Notably, treatment of MA-EVs significantly boosted the number and size of organoids while organoids treated with BA-EVs remained at a similar level with the PBS control group (Fig. 1G).

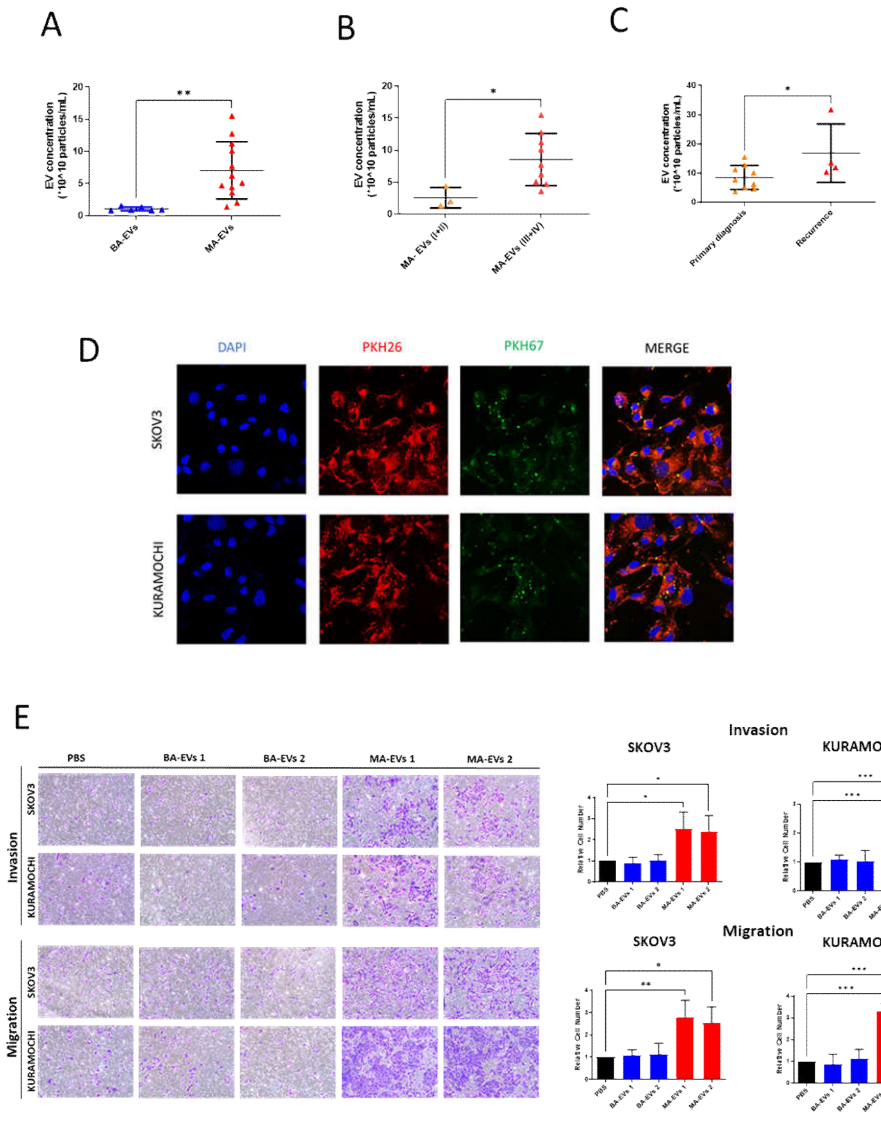
A
B
C
EV concentration (*10^10 particles/mL)
BA-EVs
MA-EVs
MA- EVs (I+II)
MA-EVs (III+IV)
Primary diagnosis
Recurrence
D
DAPI
PKH26
PKH67
MERGE
SKOV3
KURAMOCHI
E
PBS
BA-EVs 1
BA-EVs 2
MA-EVs 1
MA-EVs 2
Invasion
Migration
Relative Cell Number

F

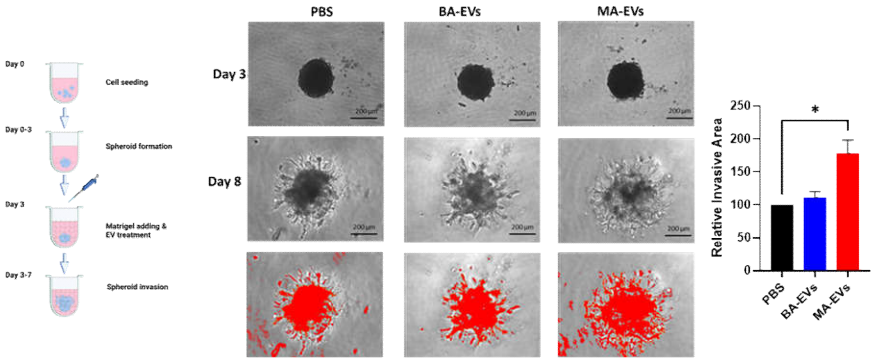
Day 0
Cell seeding
Day 0-3
Spheroid formation
Day 3
Matrigel adding &
EV treatment
Day 3-7
Spheroid invasion
PBS
BA-EVs
MA-EVs
Day 3
Day 8
Relative Invasive Area
250
200
150
100
50
0
*
PBS
BA-EVs
MA-EVs

G

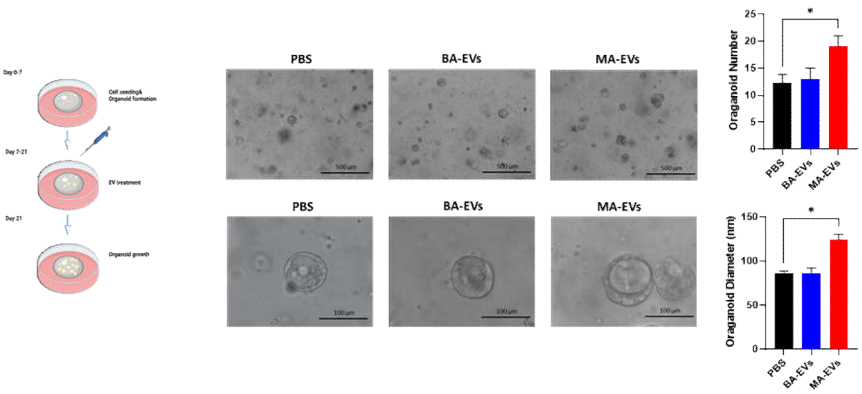
Day 0-7
Cell seeding&
Organoid formation
Day 7-21
EV treatment
Day 21
Organoid growth
PBS
BA-EVs
MA-EVs
PBS
BA-EVs
MA-EVs
Oraganoid Number
25
20
15
10
5
0
*
PBS
BA-EVs
MA-EVs
Oraganoid Diameter (nm)
150
100
50
0
*
PBS
BA-EVs
MA-EVs

Fig. 1. Alterations of ovarian cancer malignant phenotypes with MA-EVs treatment.

A. Concentration of BA-EVs and MA-EVs determined by NTA.

B. Concentration of MA-EVs (stage I+II) and MA-EVs (stage III+IV).

C. Concentration of MA-EVs (primary diagnosis) and MA-EVs (recurrence).

D. EV uptake by cancer cells. Cancer cell membranes were stained with PKH26 in red while MA-EVs were stained with PKH-67 in green. Uptake of MA-EVs by SKOV3 and KURAMOCHI were detected by confocal microscopy.

E. Ovarian cells were treated with MA-EVs or BA-EVs and the invasive and migratory ability were determined by transwell assay.

F. 3D invasion assay. Primary ascites cells (A37) were seeded in the Ultra-Low Attachment 96 well-plate to form spheroids. Three days later, EVs in Matrigel were added to mature spheroids for another five days' culture. Invasion of cancer cells into Matrigel was observed by microscopy.

G. Ascites cell-derived organoids were established to assess the effect of MA-EVs. Ascites cells were seeded in the Matrigel to form organoids. Then, fourteen-day-old organoids were treated with PBS, BA-EVs or MA-EVs continuously for 2 weeks. The number and size

of organoids were assessed after EV treatment. *, $P < 0.05$; **, $P < 0.01$; ***, $P < 0.001$.

3.2. Hypoxic condition-induced upregulation of miR-1246 and miR-1290 from malignant ascites-derived EVs is in parallel with the enhancement of ovarian cancer cell invasion and migration

The EV miRNA signature could not only serve as a clinical biomarker in liquid biopsy but also intensively influence cancer hallmarks. Next, we aimed to identify the functional miRNAs shuttled in MA-EVs involved in altering ovarian cancer metastatic ability. miR-1246 and miR-1290 were chosen as target miRNAs for ulterior analysis as they were among the most upregulated miRNAs in malignant samples and the absolute expression levels of these two miRNAs were remarkably high (Fig. S1A, B). The treatment of malignant ascites-derived EVs could significantly increase the level of miR-1246 and miR-1290 in SKOV3 and KURAMOCHI cells, indicating these two miRNAs could be transported into the recipient cells (Fig. S1C).

The expression of miR-1246 and miR-1290 in the ascites and plasma subset were illustrated in the heatmaps (Fig. 2A, B). To further investigate the expression pattern of miR-1246 and miR-1290, we carried out RT-qPCR using a larger scale of clinical samples. The level of these two miRNAs was significantly elevated in MA-EVs and MP-EVs compared to the benign counterparts (Fig. 2C, D). Noticeably, miR-1246 and miR-1290 upregulation was observed

even in early-stage (stage I+II) cancer patients (Fig. 5E). The expression of miR-1246 and miR-1290 were shown to be negatively related with patient survival in the public dataset (Fig. S1D). Here, the survival analysis in our study demonstrated that plasma EV miR-1290 level was strongly associated with patient overall survival (OS) and progression-free survival (PFS) while EV miR-1246 expression showed no correlation with patient survival, indicating the potential prognosis predictive value of miR-1290 (Fig. S1E, F).

As the expression of miR-1246 and miR-1290 was strongly augmented in malignant biofluids, we wondered if this tendency resulted from the discrepant secretion between cancer cells and normal epithelial cells. Therefore, we analyzed the expression of miR-1246 and miR-1290 in cancer cells and normal epithelial cells as well as the respective EVs using the miRNA profiling data in the GSE103708. However, no significant difference was observed between the normal and cancer group neither in the cell level nor in the EV level (Fig. S2A). In addition, EV miR-1290 was reported to discriminate HGSOC patients from those with other ovarian cancer histological types (143). However, no difference in miR-1246 or miR-1290 expression was detected between HGSOC and non-HGSOC cell lines or respective EVs (Fig S2A). Notably, the expression of miR-1246 and miR-1290 in cells and respective EVs

were not correlated, indicating a complicated sorting mechanism might be involved in the secretion process of these two miRNAs (Fig. S2B). Besides, the cellular and EV expression pattern of miR-145-5p, miR-34c-5p, miR-429, miR-145-5p included in the OCEM signature (miR-34b-3p and miR-449a were not available in GSE103708) was also demonstrated in Fig. S2E, F, G, H, I, J, K, L.

As hypoxia is one of the pivotal hallmarks of cancer, we then investigated if hypoxia could cause an alteration in the expression of miR-1246 and miR-1290 in EVs. SKOV3 and KURAMOCHI cells were cultured in media supplemented with EV-free FBS in normoxic and hypoxic conditions. EVs were isolated from the conditioned media and identified as double-membrane particles ranging from 30 nm to 200 nm positive with CD63 and CD9 expression through TEM, NTA and western blotting (Fig. 2F, G, H). Intriguingly, the expression of miR-1246 and miR-1290 was dramatically elevated in hypoxic EVs (H-EVs) than normoxic EVs (N-EVs) (Fig. 2I, J).

Subsequently, we investigated the impact of these two miRNAs on the invasive and migratory ability of ovarian cancercells. As shown in Fig. 2K, inhibition of miR-1246 and miR-1290 conspicuously suppressed the invasion and migration of SKOV3 and KURAMOCHI cells, whereas overexpression of these two miRNAs showed the opposite effect. During ovarian cancer metastatic spread,

the omentum is one of the most preferred sites of the transcoelomic metastasis. Therefore, we developed an ex vivo model using the ovarian cancer patient-derived omentum adipose tissues to further investigate the impact of miR-1246 and miR-1290 on the ovarian cancer migratory ability. Consistently, SKOV3^{luc} transfected with miR-1246 or miR-1290 inhibitors having migrated to the omentum tissue pieces showed a decreased luminescence intensity than the control group while those transfected with miR-1246 or miR-1290 mimics exhibited an augmented luminescence intensity. These results demonstrated that miR-1246 and miR-1290 encapsulated in MA-EVs played a critical role in facilitating the invasion and migration of ovarian cancer cells.

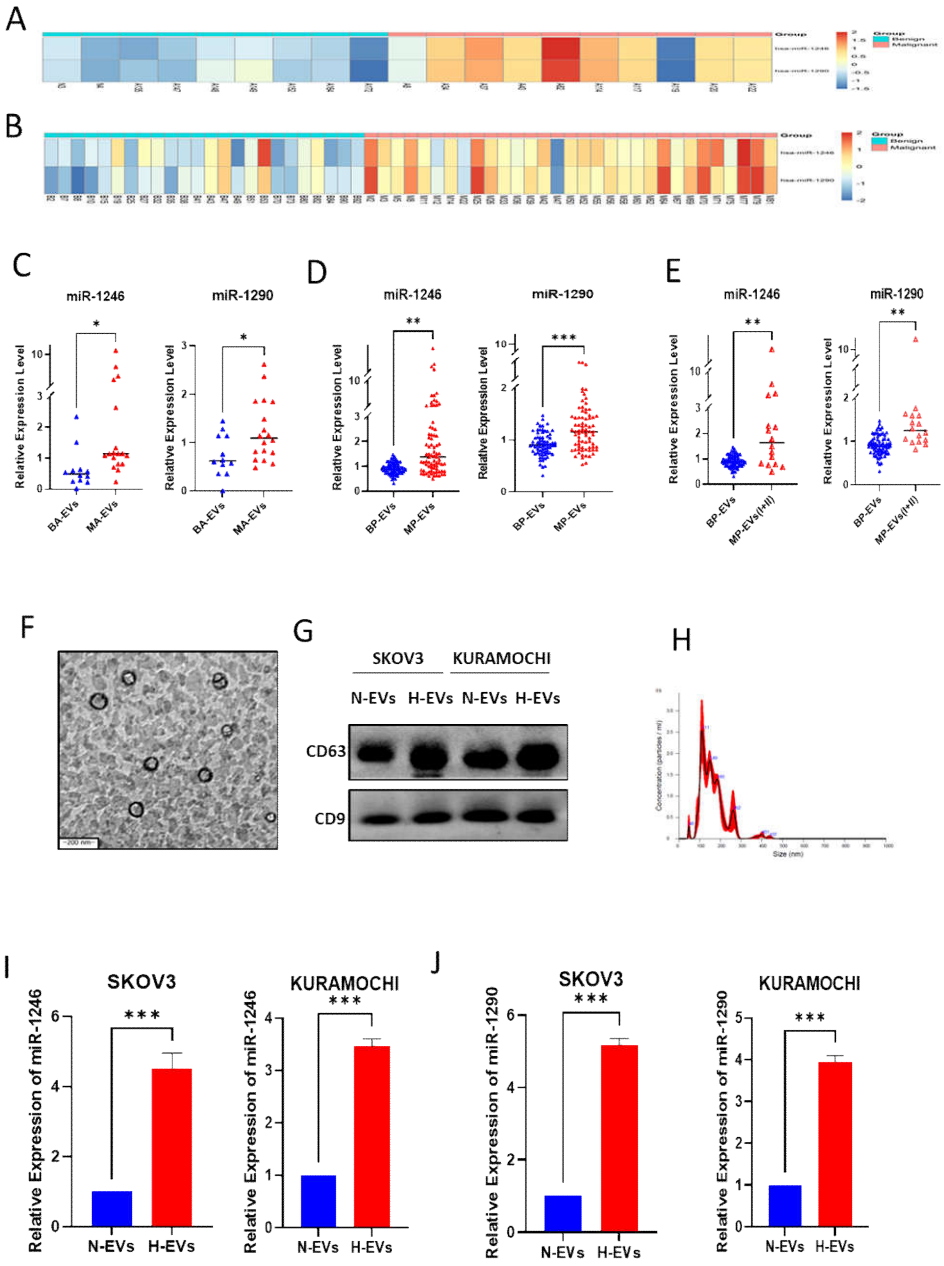
A
B
C
miR-1246
miR-1290
Relative Expression Level
BA-EVs
MA-EVs
D
BP-EVs
MP-EVs
E
MP-EVs(HI)
F
G
SKOV3
KURAMOCHI
N-EVs H-EVs N-EVs H-EVs
CD63
CD9
H
I
Relative Expression of miR-1246
J
Relative Expression of miR-1290

K

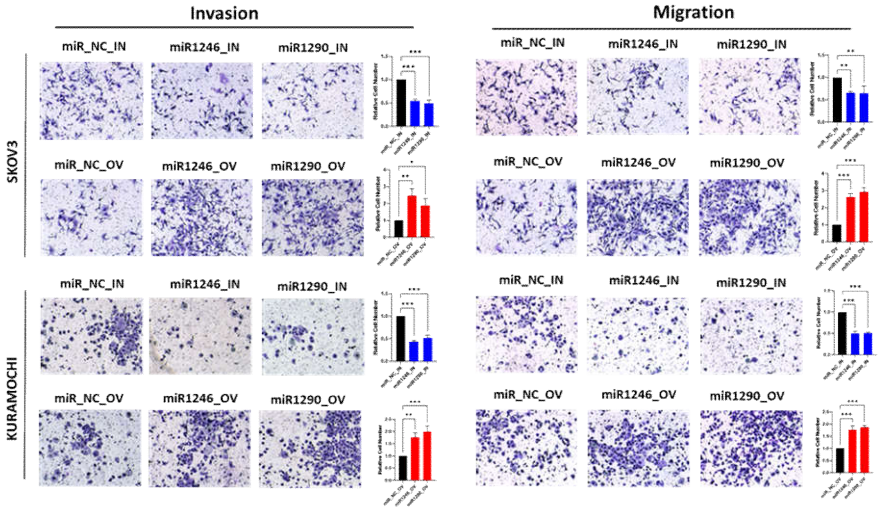
Invasion
Migration
SKOV3
KURAMOCHI
miR_NC_IN
miR1246_IN
miR1290_IN
miR_NC_OV
miR1246_OV
miR1290_OV

L

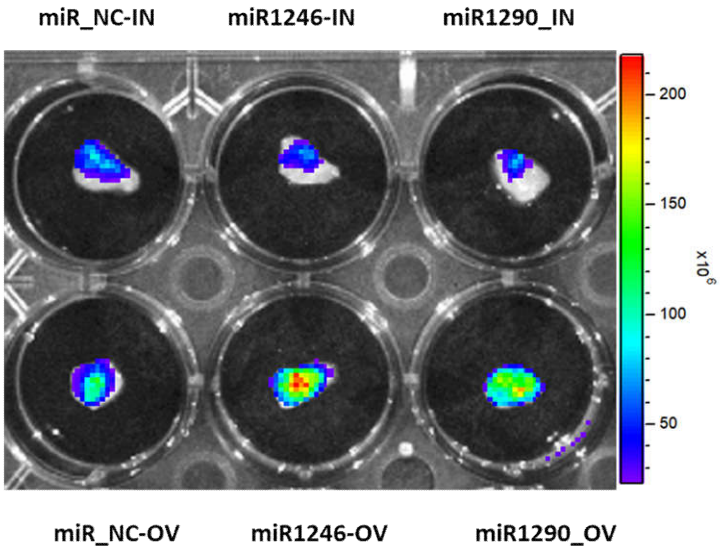
miR_NC-IN
miR1246-IN
miR1290_IN
200
150
100
50
X10⁶
miR_NC-OV
miR1246-OV
miR1290_OV

Fig. 2. The impact of miR-1246 and miR-1290 shuttled in MA-EVs on the metastatic potential of ovarian cancer cells.

A. The heatmap showed the expression of miR-1246 and miR-1290 in the ascites subset.

B. The heatmap demonstrated the expression of miR-1246 and miR-1290 in the plasma subset.

C. Expression of miR-1246 and miR-1290 was measured in MA-EVs (N=18) and BA-EVs (N=12) by RT-qPCR.

D. Expression of miR-1246 and miR-1290 was measured in MP-EVs (N=78 and BP-EVs (N=72) by RT-qPCR.

E. Comparison of MiR-1246 and miR-1290 expression in early-stage (stage I+II) cancer patient MP-EVs (N=16) and BP-EVs (N=72). EVs were isolated from cancer cell culture media.

F. TEM was performed to identify the morphology of cancer cell line-derived EVs.

G. Western blotting was carried out to detect EV marker CD63 and CD9 expression of cancer cell line-derived EVs.

H. NTA was used to identify size contribution and concentration of cancer cell line-derived EVs.

I. Expression of miR-1246 in hypoxic and normoxic EVs.

J. Expression of miR-1290 in hypoxic and normoxic EVs.

K. MiRNA inhibitors or mimics were treated to ovarian cancer

cells were treated with to investigate their effect on ovarian cancer invasion and migration. H-EVs: hypoxic EVs; N-EVs: normoxic EVs; IN: inhibition; OV: overexpression. *, $P < 0.05$; **, $P < 0.01$; ***, $P < 0.001$.

L, Ovarian cancer patient-derived omentum adipose tissues were coculture with SKOV3luc cells with different miRNA inhibitors or mimics for 5 days. The number of SKOV3luc cells having migrated to the omentum tissue pieces was determined by the luminescence intensity measured with IVIS 100 imaging system.

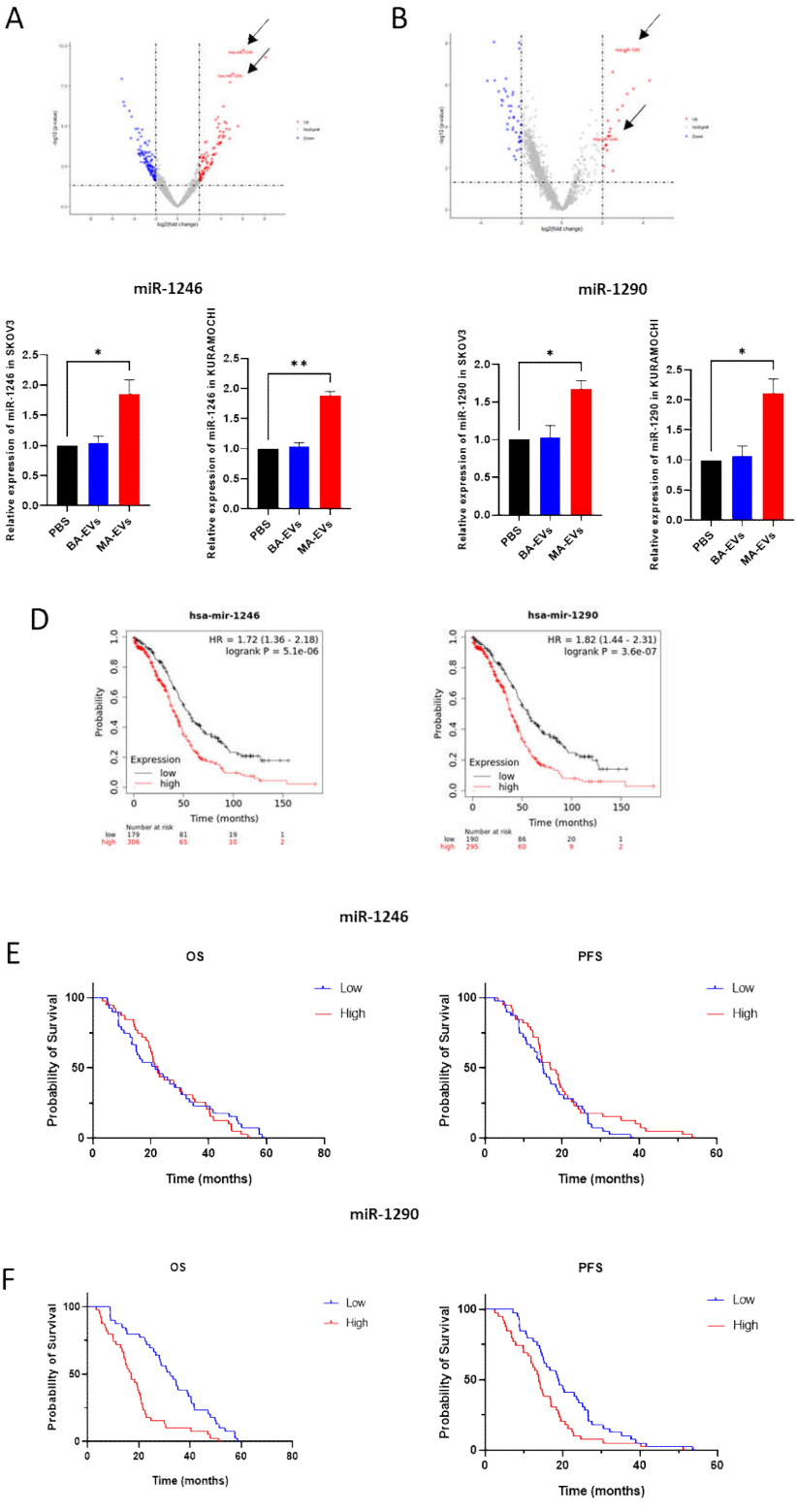
A
B
C
miR-1246
miR-1290
Relative expression of miR-1246 in SKOV3
Relative expression of miR-1246 in KURAMOCHI
Relative expression of miR-1290 in SKOV3
Relative expression of miR-1290 in KURAMOCHI
PBS
BA-EVs
MA-EVs
D
hsa-mir-1246
HR = 1.72 (1.36 - 2.18)
logrank P = 5.1e-06
hsa-mir-1290
HR = 1.82 (1.44 - 2.31)
logrank P = 3.6e-07
Probability
Expression
low
high
Time (months)
Number at risk
miR-1246
E
OS
PFS
Low
High
Probability of Survival
Time (months)
miR-1290
F

Fig. S1. The volcano plots showed that miR-1246 and miR-1290 were among the most significant DEmiRs in ascites (A) and plasma subset (B). C. The expression of miR-1246 and miR-1290 in SKOV3 and KURAMOCHI cells after treated with PBS, BA-EVs and MA-EVs. D. The correlation of tissue expression of miR-1246 and miR-1290 with the patient OS by the online tool Kaplan Meier plotter. E. The association of plasma EV miR-1246 expression and patient OS and PFS. E. The association of plasma EV miR-1246 expression and patient OS and PFS. F. The association of plasma EV miR-1290 expression and patient OS and PFS.

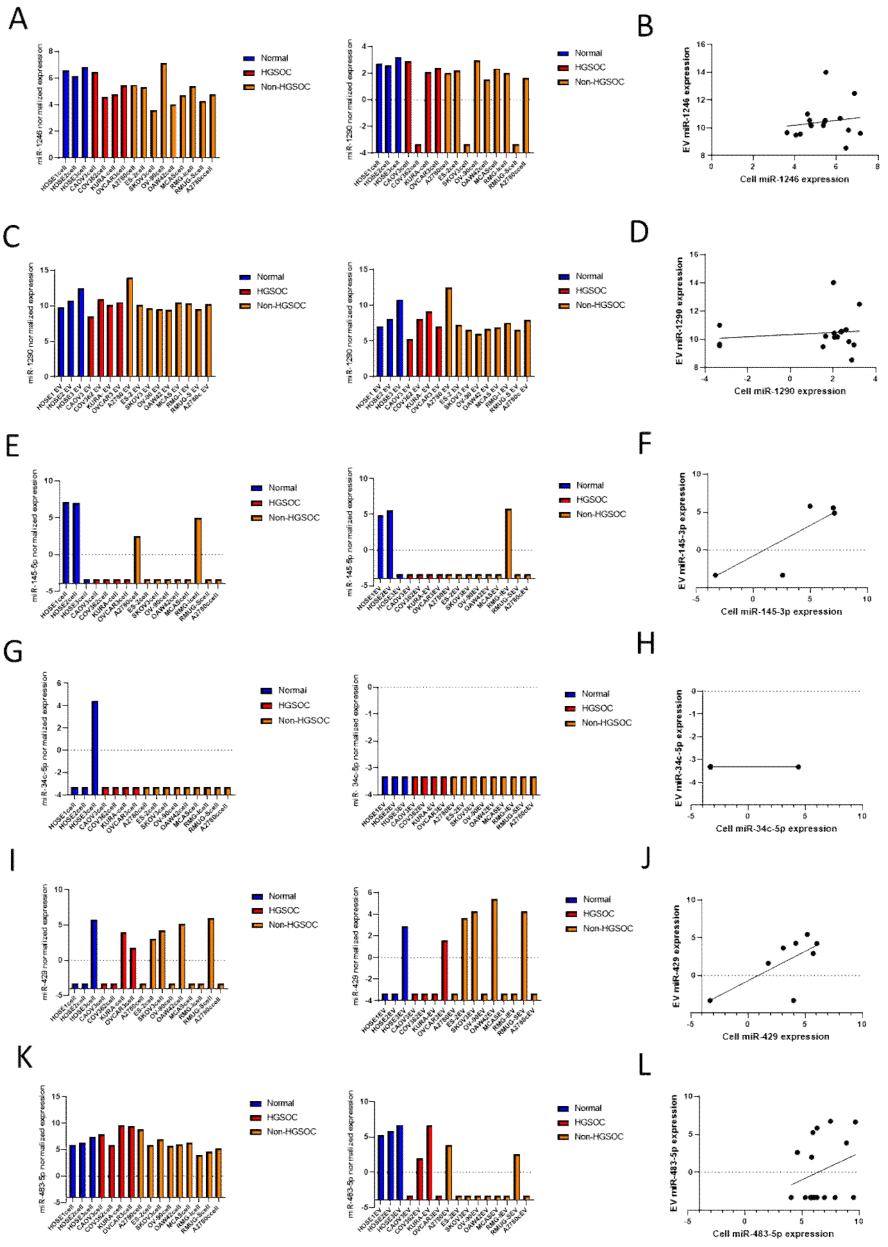

M

miRNA\EV origin cell	NF-1	NF-2	CAF-1	CAF-2	NA-1	NA-2	CAA-1	CAA-2
miR-1246	+	-	-	+	+	+	+	-
miR-1290	-	+	-	+	-	-	+	-
miR-483	-	+	-	-	-	-	-	-
miR-429	-	-	-	-	-	-	+	-
miR-34b-3p	-	-	-	-	-	-	-	-
miR-34c-5p	-	-	-	+	-	-	+	-
miR-145-5p	+	+	-	-	+	+	-	+
miR-449a	-	-	-	-	-	-	-	-

Fig. S2. The cellular and EV expression of miR-1246 (A), miR-1290 (C), miR-145-5p (E), miR-34c-5p (G), miR-429 (I), miR-145-5p (K) in the OCEM signature in normal cell lines and cancer (HGSOC and non-HGSOC) cell lines in the GSE103708. The correlation of miR-1246 (B), miR-1290 (D), miR-145-5p (F), miR-34c-5p (H), miR-429 (J), miR-145-5p (L) in cells and respective EVs. M. The expression of eight miRNAs in the OCEM signature in non-cancer cell-derived EVs in the GSE77318 dataset. +: miRNA expression >= 1 counts per 1000 cells; -: miRNA expression <= 1 counts per 1000 cells or miRNA data not available. NF: normal fibroblast; CAF: cancer-associated fibroblast; NA: normal adipocyte; CAA: cancer-associated adipocyte.

3.3. RORα was identified as a common target of miR-1246 and miR-1290, exerting the tumor suppressive function in ovarian cancer

Since miR-1246 and miR-1290 share similar sequences, they are supposed to be capable of binding to some common targets. We used the online tool to predict the common targets of miR-1246 and miR-1290 (Fig.3A). Among the ten predicted targets, retinoid orphan receptor alpha (RORα) was the only one evidently downregulated in ovarian cancer tissues than normal tissues in GEPIA (Fig. 3B). Therefore, we selected RORα as a potential target for validation by western blotting and luciferase reporter gene assay. The result showed that inhibition of miR-1246 and miR-1290 could significantly augment the expression of RORα in SKOV3 and KURAMOCHI cells (Fig. 3C). Then, the RORα 3′ -UTR sequence containing the putative miRNA target region in the wild form (WT) or mutated form with putative binding region altered (MT) was constructed (Fig. 3D). The luciferase activity was remarkably decreased only in cells co-transfected with RORα WT and miR-1246 or miR-1290 mimics, indicating that miR-1246 and miR-1290 could directly regulate RORα through binding to its 3′ -UTR (Fig. 3E). We further investigated the function of RORα in ovarian cancer. Overexpression of RORα in ovarian cancer cells conspicuously impeded their invasive and migratory ability (Fig. 3F). Moreover, this inhibitory

effect could be antagonized by the simultaneous miR-1246 or miR-1290 overexpression (Fig. 3G). In addition, the IHC assay (HGSOC tissues: N=58) was performed to explore the clinical significance of RORα. The higher expression of RORα was related to a longer OS while the lower expression was associated with a shorter OS in HGSOC patients (Fig. 3H, I). These results suggested that RORα could act as a tumor-suppressive gene in ovarian cancer.

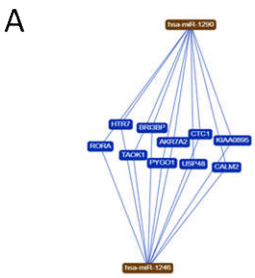
A
hsa-miR-1290
HTR7
BRSK2
CTC1
KIAA0895
RORA
AKR1A2
TACR1
PYGO1
USP48
CALM2
hsa-miR-1246

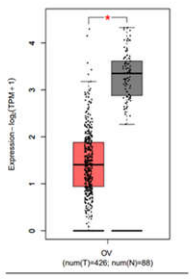
B
Expression - log2(TPM + 1)
OV
(num(T)=426; num(N)=88)

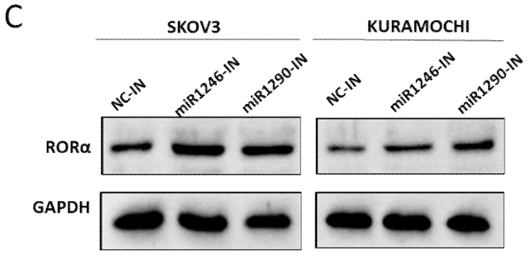
C
SKOV3
KURAMOCHI
NC-IN
miR1246-IN
miR1290-IN
NC-IN
miR1246-IN
miR1290-IN
RORα
GAPDH


D
RORA 3' UTR MT
- AAAAUCCA-
miR-1246
GGACGAGGUUUUUAGGUAA
miR-1290
AGGGACUAGGUUUUUAGGU
XXXXXXXXX
RORA 3' UTR WT
- UUGGAAUC-

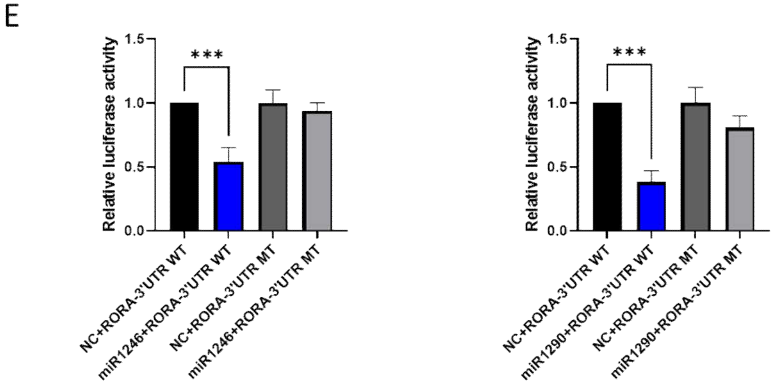
E
Relative luciferase activity
1.5
1.0
0.5
0.0
***
NC+RORA-3'UTR WT
miR1246+RORA-3'UTR WT
NC+RORA-3'UTR MT
miR1246+RORA-3'UTR MT
Relative luciferase activity
1.5
1.0
0.5
0.0
***
NC+RORA-3'UTR WT
miR1290+RORA-3'UTR WT
NC+RORA-3'UTR MT
miR1290+RORA-3'UTR MT

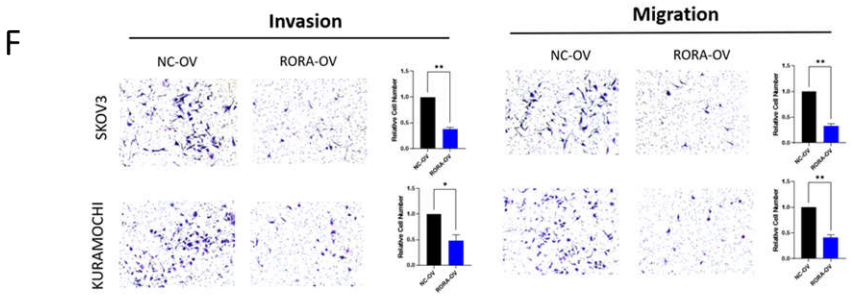
F
Invasion
Migration
NC-OV
RORA-OV
NC-OV
RORA-OV
SKOV3
KURAMOCHI

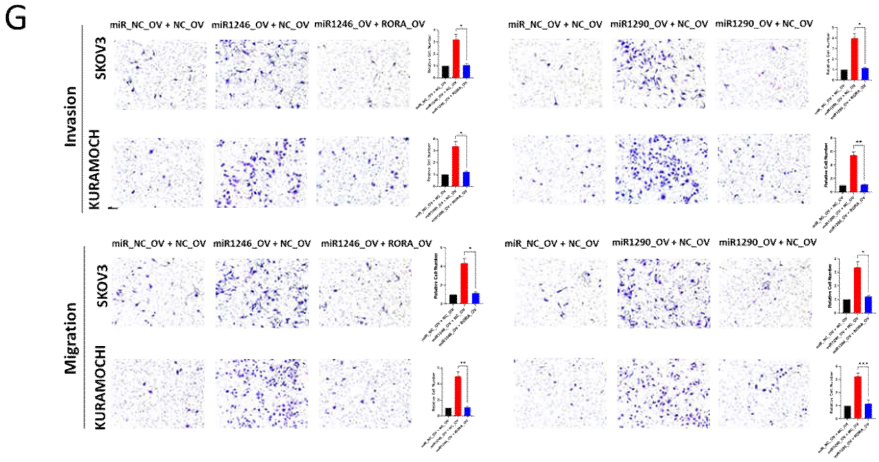
G
Invasion
Migration
SKOV3
KURAMOCHI
miR_NC_OV + NC_OV
miR1246_OV + NC_OV
miR1246_OV + RORA_OV
miR1290_OV + NC_OV

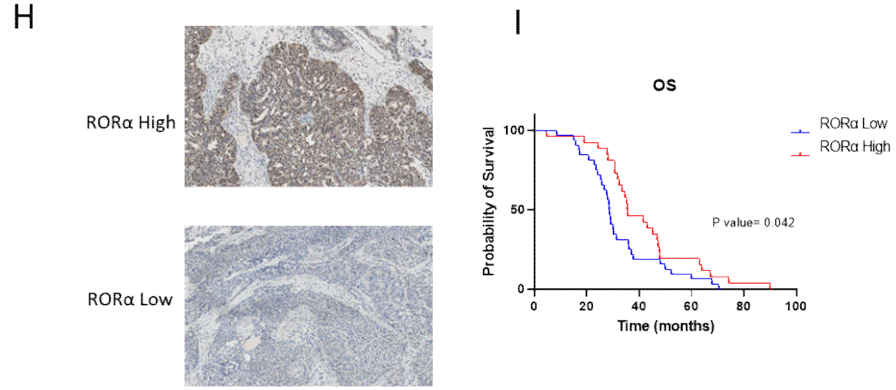
H
RORα High
RORα Low
I
OS
RORα Low
RORα High
Probability of Survival
P value= 0.042
Time (months)

Fig. 3. RORα identified as a common downstream target of miR-1246 and miR-1290.

A. Common targets of miR-1246 and miR-1290 were predicted using the online tool.

B. Expression of RORα in ovarian cancer tissues and normal tissues in GEPIA (http://gepia.cancer-pku.cn/).

C. The alteration of RORα expression in SKOV3 and KURAMOCHI cells with the inhibition of miR-1246 and miR-1290 was determined by Western blotting.

D. The putative miRNA target region in the RORα 3′ -UTR wild form (WT) or mutated form with putative binding region altered (MT) was constructed.

E. Dual-luciferase reporter gene assay was performed to validate the putative binding region of miR-1246 and miR-1290 with RORα 3′ -UTR.

F. The invasive and migratory ability of ovarian cancer cells when overexpressed with RORα was measured.

G. The rescue experiment was carried out to investigate if miR-1246 or miR-1290 could restore the effect in ovarian cancer invasion and migration by RORα overexpression.

H. RORα in ovarian cancer tissues and normal tissues was analyzed.

I. IHC assay was performed to investigate the relation between tissue RORα expression and overall survival in HGSOC patients. OV: overexpression. *, $P < 0.05$; **, $P < 0.01$; ***, $P < 0.001$.

4. Discussion

EVs propagate phenotypic traits to recipient cells by transferring multiple molecular cargoes. MA-EVs are intimately in contact with the primary tumor and secondary metastasis, actively mediating the cellular interactions in the peritoneal cavity. Our results elucidated that MA-EVs play a critical role in facilitating ovarian cancer metastasis. Noticeably, we established organoids from primary cells in the ascites better mimicking the histopathological features and molecular patterns of the original tumor. Then, we innovatively treated MA-EVs to these organoids and found that MA-EVs significantly boosted the growth of organoids. A previous research in gastric cancer reported that the centrifuged supernatant of ascites could promote the proliferation of ascites-derived organoids (154). However, they did not clarify the functional substances attributed to this effect. To our knowledge, we are the first to have demonstrated the impact of ascites-derived EVs on the growth of organoids. The subsequential analysis identified that MA-EVs exerted their pro-aggressive effect through transferring functional miRNAs. Analysis using the public dataset revealed that representative miRNAs could not only detected in epithelial cells or cancer cells but also in stromal cells including fibroblasts and adipocytes (Fig. S7E), indicating these miRNAs might play an important role in regulating

the cancer-cancer, cancer-stromal, stromal-stromal cell communication in the ascites tumor microenvironment. Here we focused on the impact of MA-EV miRNAs on the malignant behaviors of cancer cells in this study. Researches on exploring the role of MA-EVs and MA-EV miRNAs in mediating cancer-stromal interactions might shed new light on deeper comprehension of the tumor microenvironment in the ascites. miR-1246 and miR-1290 were chosen for ulterior analysis as they were among the most upregulated miRNAs in malignant samples and the absolute expression levels of these two miRNAs were remarkably high. Previous studies reported that miR-1246 and miR-1290 were associated with tumor proliferation, metastasis, stemness or therapy resistance by regulating various downstream targets in lung cancer (155-157), oral squamous cell carcinoma (158), breast cancer (159), gastric cancer (160), esophageal squamous cell carcinoma (161) and pancreatic cancer (162), etc. Here we demonstrated that miR-1246 and miR-1290 shuttled in MA-EVs could induce the invasion and migration of ovarian cancer cells. Besides, cancer and non-cancer cells in the ascites can form multicellular aggregates or spheroids, where the core is usually hypoxic (149). As a featured hallmark of cancer, hypoxia was reported to profoundly impact the cell fate and EV secretion. Our result showed that hypoxia could induce the

expression miR-1246 and miR-1290, which was consistent with the previous reports in other cancer types (163, 164). Subsequently, we identified RORα as a common downstream target of miR-1246 and miR-1290. RORα is known as a tumor suppressor that has been reported to inhibit tumorigenesis, tumor proliferation and metastasis in glioma (165), oral squamous cell carcinoma (166) and breast cancer (167). Based on the pro-aggressive function of miR-1246 and miR-1290 in ovarian cancer, inhibiting these two miRNAs might be a novel therapeutic strategy. Currently, there are mainly three ways to attain the miRNA loss of function: miRNA sponges, antisense oligonucleotides and Clustered Regularly Interspaced Short Palindromic Repeats/CRISPR-associated protein 9 (CRISPR/Cas9)-based gene editing technologies (168-170). Recent advances have addressed the therapeutic value of miRNAs and the possible clinical translational potential in ovarian cancer treatment (171-174). However, there are a set of challenges to be overcome before miRNA-based therapies can be brought from bench to the bedside, including delivery systems, toxicity concerns, administration routes, off-target effects, etc. (170).

References

1. Dayan F, Mazure NM, Brahimi-Horn MC, Pouyssegur J. A dialogue between the hypoxia-inducible factor and the tumor microenvironment. Cancer Microenviron. 2008;1(1):53-68.
2. Waldmann TA. Cytokines in Cancer Immunotherapy. Cold Spring Harb Perspect Biol. 2018;10(12).
3. Cadamuro M, Brivio S, Spirli C, Joplin RE, Strazzabosco M, Fabris L. Autocrine and Paracrine Mechanisms Promoting Chemoresistance in Cholangiocarcinoma. Int J Mol Sci. 2017;18(1).
4. Wegiel B, Vuerich M, Daneshmandi S, Seth P. Metabolic Switch in the Tumor Microenvironment Determines Immune Responses to Anti-cancer Therapy. Front Oncol. 2018;8:284.
5. Jing X, Yang F, Shao C, Wei K, Xie M, Shen H, et al. Role of hypoxia in cancer therapy by regulating the tumor microenvironment. Mol Cancer. 2019;18(1):157.
6. Kuchuk O, Tuccitto A, Citterio D, Huber V, Camisaschi C, Milione M, et al. pH regulators to target the tumor immune microenvironment in human hepatocellular carcinoma. Oncoimmunology. 2018;7(7):e1445452.
7. Lim B, Woodward WA, Wang X, Reuben JM, Ueno NT. Inflammatory breast cancer biology: the tumour microenvironment is key. Nat Rev Cancer. 2018;18(8):485-99.
8. Weinberg F, Ramnath N, Nagrath D. Reactive Oxygen Species in the Tumor Microenvironment: An Overview. Cancers (Basel). 2019;11(8).
9. Casazza A, Di Conza G, Wenes M, Finisguerra V, Deschoemaeker S, Mazzone M. Tumor stroma: a complexity dictated by the hypoxic tumor microenvironment. Oncogene. 2014;33(14):1743-54.
10. Campbell EJ, Dachs GU, Morrin HR, Davey VC, Robinson BA, Vissers MCM. Activation of the hypoxia pathway in breast cancer tissue and patient survival are inversely associated with tumor ascorbate levels. BMC Cancer. 2019;19(1):307.
11. Erkan M, Kurtoglu M, Kleeff J. The role of hypoxia in pancreatic cancer: a potential therapeutic target? Expert Rev Gastroenterol Hepatol. 2016;10(3):301-16.
12. Han Y, Kim B, Cho U, Park IS, Kim SI, Dhanasekaran DN, et al. Mitochondrial fission causes cisplatin resistance under hypoxic conditions via ROS in ovarian cancer cells. Oncogene. 2019;38(45):7089-105.
13. Salem A, Asselin MC, Reymen B, Jackson A, Lambin P, West CML, et al. Targeting Hypoxia to Improve Non-Small Cell Lung Cancer Outcome. J Natl Cancer Inst. 2018;110(1).
14. Yang L, Roberts D, Takhar M, Erho N, Bibby BAS, Thiruthaneeswaran N, et al. Development and Validation of a 28-gene Hypoxia-related Prognostic Signature for Localized Prostate Cancer. EBioMedicine. 2018;31:182-9.
15. Petrova V, Annicchiarico-Petruzzelli M, Melino G, Amelio I. The hypoxic tumour microenvironment. Oncogenesis. 2018;7(1):10.

16. Akanji MA, Rotimi D, Adeyemi OS. Hypoxia-Inducible Factors as an Alternative Source of Treatment Strategy for Cancer. Oxid Med Cell Longev. 2019;2019:8547846.
17. McKeown SR. Defining normoxia, physoxia and hypoxia in tumours-implications for treatment response. Br J Radiol. 2014;87(1035):20130676.
18. Camuzi D, de Amorim ISS, Ribeiro Pinto LF, Oliveira Trivilin L, Mencalha AL, Soares Lima SC. Regulation Is in the Air: The Relationship between Hypoxia and Epigenetics in Cancer. Cells. 2019;8(4).
19. Kang J, Shin SH, Yoon H, Huh J, Shin HW, Chun YS, et al. FIH Is an Oxygen Sensor in Ovarian Cancer for G9a/GLP-Driven Epigenetic Regulation of Metastasis-Related Genes. Cancer Res. 2018;78(5):1184-99.
20. Li Y, Patel SP, Roszik J, Qin Y. Hypoxia-Driven Immunosuppressive Metabolites in the Tumor Microenvironment: New Approaches for Combinational Immunotherapy. Front Immunol. 2018;9:1591.
21. Tawadros AIF, Khalafalla MMM. Expression of programmed death-ligand 1 and hypoxia-inducible factor-1alpha proteins in endometrial carcinoma. J Cancer Res Ther. 2018;14(Supplement):S1063-S9.
22. Noman MZ, Desantis G, Janji B, Hasmim M, Karray S, Dessen P, et al. PD-L1 is a novel direct target of HIF-1alpha, and its blockade under hypoxia enhanced MDSC-mediated T cell activation. J Exp Med. 2014;211(5):781-90.
23. Deng J, Li J, Sarde A, Lines JL, Lee YC, Qian DC, et al. Hypoxia-Induced VISTA Promotes the Suppressive Function of Myeloid-Derived Suppressor Cells in the Tumor Microenvironment. Cancer Immunol Res. 2019;7(7):1079-90.
24. Daniel SK, Sullivan KM, Labadie KP, Pillarisetty VG. Hypoxia as a barrier to immunotherapy in pancreatic adenocarcinoma. Clin Transl Med. 2019;8(1):10.
25. Kugeratski FG, Atkinson SJ, Neilson LJ, Lilla S, Knight JRP, Serneels J, et al. Hypoxic cancer-associated fibroblasts increase NCBP2-AS2/HIAR to promote endothelial sprouting through enhanced VEGF signaling. Sci Signal. 2019;12(567).
26. De Francesco EM, Lappano R, Santolla MF, Marsico S, Caruso A, Maggiolini M. HIF-1alpha/GPER signaling mediates the expression of VEGF induced by hypoxia in breast cancer associated fibroblasts (CAFs). Breast Cancer Res. 2013;15(4):R64.
27. Hirakawa T, Yashiro M, Doi Y, Kinoshita H, Morisaki T, Fukuoka T, et al. Pancreatic Fibroblasts Stimulate the Motility of Pancreatic Cancer Cells through IGF1/IGF1R Signaling under Hypoxia. PLoS One. 2016;11(8):e0159912.
28. Andersen S, Richardsen E, Moi L, Donnem T, Nordby Y, Ness N, et al. Fibroblast miR-210 overexpression is independently associated with clinical failure in Prostate Cancer - a multicenter (in situ hybridization) study. Sci Rep. 2016;6:36573.
29. S ELA, Mager I, Breakefield XO, Wood MJ. Extracellular vesicles: biology and emerging therapeutic opportunities. Nat Rev Drug Discov. 2013;12(5):347-57.
30. Zhang Y, Liu Y, Liu H, Tang WH. Exosomes: biogenesis, biologic

function and clinical potential. Cell Biosci. 2019;9:19.
31. Henne WM, Buchkovich NJ, Emr SD. The ESCRT pathway. Dev Cell. 2011;21(1):77-91.
32. Eldh M, Ekstrom K, Valadi H, Sjostrand M, Olsson B, Jernas M, et al. Exosomes communicate protective messages during oxidative stress; possible role of exosomal shuttle RNA. PLoS One. 2010;5(12):e15353.
33. Kim KM, Abdelmohsen K, Mustapic M, Kapogiannis D, Gorospe M. RNA in extracellular vesicles. Wiley Interdiscip Rev RNA. 2017;8(4).
34. Bang C, Thum T. Exosomes: new players in cell-cell communication. Int J Biochem Cell Biol. 2012;44(11):2060-4.
35. Berchem G, Noman MZ, Bosseler M, Paggetti J, Baconnais S, Le Cam E, et al. Hypoxic tumor-derived microvesicles negatively regulate NK cell function by a mechanism involving TGF-beta and miR23a transfer. Oncoimmunology. 2016;5(4):e1062968.
36. Chen X, Ying X, Wang X, Wu X, Zhu Q, Wang X. Exosomes derived from hypoxic epithelial ovarian cancer deliver microRNA-940 to induce macrophage M2 polarization. Oncol Rep. 2017;38(1):522-8.
37. Tadokoro H, Umezu T, Ohyashiki K, Hirano T, Ohyashiki JH. Exosomes derived from hypoxic leukemia cells enhance tube formation in endothelial cells. J Biol Chem. 2013;288(48):34343-51.
38. Yin Y, Cai X, Chen X, Liang H, Zhang Y, Li J, et al. Tumor-secreted miR-214 induces regulatory T cells: a major link between immune evasion and tumor growth. Cell Res. 2014;24(10):1164-80.
39. Yang M, Chen J, Su F, Yu B, Su F, Lin L, et al. Microvesicles secreted by macrophages shuttle invasion-potentiating microRNAs into breast cancer cells. Mol Cancer. 2011;10:117.
40. Au Yeung CL, Co NN, Tsuruga T, Yeung TL, Kwan SY, Leung CS, et al. Exosomal transfer of stroma-derived miR21 confers paclitaxel resistance in ovarian cancer cells through targeting APAF1. Nat Commun. 2016;7:11150.
41. Lasser C, Alikhani VS, Ekstrom K, Eldh M, Paredes PT, Bossios A, et al. Human saliva, plasma and breast milk exosomes contain RNA: uptake by macrophages. J Transl Med. 2011;9:9.
42. El-Andaloussi S, Lee Y, Lakhal-Littleton S, Li J, Seow Y, Gardiner C, et al. Exosome-mediated delivery of siRNA in vitro and in vivo. Nat Protoc. 2012;7(12):2112-26.
43. Haney MJ, Klyachko NL, Zhao Y, Gupta R, Plotnikova EG, He Z, et al. Exosomes as drug delivery vehicles for Parkinson's disease therapy. J Control Release. 2015;207:18-30.
44. Kim SM, Yang Y, Oh SJ, Hong Y, Seo M, Jang M. Cancer-derived exosomes as a delivery platform of CRISPR/Cas9 confer cancer cell tropism-dependent targeting. J Control Release. 2017;266:8-16.
45. Saari H, Lazaro-Ibanez E, Viitala T, Vuorimaa-Laukkanen E, Siljander P, Yliperttula M. Microvesicle- and exosome-mediated drug delivery enhances the cytotoxicity of Paclitaxel in autologous prostate cancer cells. J Control Release. 2015;220(Pt B):727-37.
46. Crick F. Central dogma of molecular biology. Nature. 1970;227(5258):561-3.

47. Dahlberg AE. The functional role of ribosomal RNA in protein synthesis. Cell. 1989;57(4):525-9.
48. Wilusz JE, Sunwoo H, Spector DL. Long noncoding RNAs: functional surprises from the RNA world. Genes Dev. 2009;23(13):1494-504.
49. Holley RW, Apgar J, Everett GA, Madison JT, Marquisee M, Merrill SH, et al. Structure of a Ribonucleic Acid. Science. 1965;147(3664):1462-5.
50. Wei JW, Huang K, Yang C, Kang CS. Non-coding RNAs as regulators in epigenetics (Review). Oncol Rep. 2017;37(1):3-9.
51. Pigati L, Yaddanapudi SC, Iyengar R, Kim DJ, Hearn SA, Danforth D, et al. Selective release of microRNA species from normal and malignant mammary epithelial cells. PLoS One. 2010;5(10):e13515.
52. van Balkom BW, Eisele AS, Pegtel DM, Bervoets S, Verhaar MC. Quantitative and qualitative analysis of small RNAs in human endothelial cells and exosomes provides insights into localized RNA processing, degradation and sorting. J Extracell Vesicles. 2015;4:26760.
53. Hannafon BN, Trigoso YD, Calloway CL, Zhao YD, Lum DH, Welm AL, et al. Plasma exosome microRNAs are indicative of breast cancer. Breast Cancer Res. 2016;18(1):90.
54. Ragusa M, Statello L, Maugeri M, Barbagallo C, Passanisi R, Alhamdani MS, et al. Highly skewed distribution of miRNAs and proteins between colorectal cancer cells and their exosomes following Cetuximab treatment: biomolecular, genetic and translational implications. Oncoscience. 2014;1(2):132-57.
55. Kosaka N, Iguchi H, Hagiwara K, Yoshioka Y, Takeshita F, Ochiya T. Neutral sphingomyelinase 2 (nSMase2)-dependent exosomal transfer of angiogenic microRNAs regulate cancer cell metastasis. J Biol Chem. 2013;288(15):10849-59.
56. Iavello A, Frech VS, Gai C, Deregibus MC, Quesenberry PJ, Camussi G. Role of Alix in miRNA packaging during extracellular vesicle biogenesis. Int J Mol Med. 2016;37(4):958-66.
57. Wu C, So J, Davis-Dusenbery BN, Qi HH, Bloch DB, Shi Y, et al. Hypoxia potentiates microRNA-mediated gene silencing through posttranslational modification of Argonaute2. Mol Cell Biol. 2011;31(23):4760-74.
58. Villarroya-Beltri C, Gutierrez-Vazquez C, Sanchez-Cabo F, Perez-Hernandez D, Vazquez J, Martin-Cofreces N, et al. Sumoylated hnRNPA2B1 controls the sorting of miRNAs into exosomes through binding to specific motifs. Nat Commun. 2013;4:2980.
59. Qu L, Ding J, Chen C, Wu ZJ, Liu B, Gao Y, et al. Exosome-Transmitted lncARSR Promotes Sunitinib Resistance in Renal Cancer by Acting as a Competing Endogenous RNA. Cancer Cell. 2016;29(5):653-68.
60. Kossinova OA, Gopanenko AV, Tamkovich SN, Krasheninina OA, Tupikin AE, Kiseleva E, et al. Cytosolic YB-1 and NSUN2 are the only proteins recognizing specific motifs present in mRNAs enriched in exosomes. Biochim Biophys Acta Proteins Proteom. 2017;1865(6):664-73.
61. Rauen T, Frye BC, Wang J, Raffetseder U, Alidousty C, En-Nia A, et al. Cold shock protein YB-1 is involved in hypoxia-dependent gene transcription. Biochem Biophys Res Commun. 2016;478(2):982-7.

62. El-Naggar AM, Veinotte CJ, Cheng H, Grunewald TG, Negri GL, Somasekharan SP, et al. Translational Activation of HIF1alpha by YB-1 Promotes Sarcoma Metastasis. Cancer Cell. 2015;27(5):682-97.
63. Li Y, Zheng Q, Bao C, Li S, Guo W, Zhao J, et al. Circular RNA is enriched and stable in exosomes: a promising biomarker for cancer diagnosis. Cell Res. 2015;25(8):981-4.
64. Ostrowski M, Carmo NB, Krumeich S, Fanget I, Raposo G, Savina A, et al. Rab27a and Rab27b control different steps of the exosome secretion pathway. Nat Cell Biol. 2010;12(1):19-30; sup pp 1-13.
65. Dada LA, Novoa E, Lecuona E, Sun H, Sznajder JI. Role of the small GTPase RhoA in the hypoxia-induced decrease of plasma membrane Na,K-ATPase in A549 cells. J Cell Sci. 2007;120(Pt 13):2214-22.
66. Dorayappan KDP, Wanner R, Wallbillich JJ, Saini U, Zingarelli R, Suarez AA, et al. Hypoxia-induced exosomes contribute to a more aggressive and chemoresistant ovarian cancer phenotype: a novel mechanism linking STAT3/Rab proteins. Oncogene. 2018;37(28):3806-21.
67. King HW, Michael MZ, Gleadle JM. Hypoxic enhancement of exosome release by breast cancer cells. BMC Cancer. 2012;12:421.
68. Booth AM, Fang Y, Fallon JK, Yang JM, Hildreth JE, Gould SJ. Exosomes and HIV Gag bud from endosome-like domains of the T cell plasma membrane. J Cell Biol. 2006;172(6):923-35.
69. Panigrahi GK, Praharaj PP, Peak TC, Long J, Singh R, Rhim JS, et al. Hypoxia-induced exosome secretion promotes survival of African-American and Caucasian prostate cancer cells. Sci Rep. 2018;8(1):3853.
70. Kucharzewska P, Christianson HC, Welch JE, Svensson KJ, Fredlund E, Ringner M, et al. Exosomes reflect the hypoxic status of glioma cells and mediate hypoxia-dependent activation of vascular cells during tumor development. Proc Natl Acad Sci U S A. 2013;110(18):7312-7.
71. Hsu YL, Hung JY, Chang WA, Lin YS, Pan YC, Tsai PH, et al. Hypoxic lung cancer-secreted exosomal miR-23a increased angiogenesis and vascular permeability by targeting prolyl hydroxylase and tight junction protein ZO-1. Oncogene. 2017;36(34):4929-42.
72. Li L, Li C, Wang S, Wang Z, Jiang J, Wang W, et al. Exosomes Derived from Hypoxic Oral Squamous Cell Carcinoma Cells Deliver miR-21 to Normoxic Cells to Elicit a Prometastatic Phenotype. Cancer Res. 2016;76(7):1770-80.
73. Xue M, Chen W, Xiang A, Wang R, Chen H, Pan J, et al. Hypoxic exosomes facilitate bladder tumor growth and development through transferring long non-coding RNA-UCA1. Mol Cancer. 2017;16(1):143.
74. Boeckel JN, Jae N, Heumuller AW, Chen W, Boon RA, Stellos K, et al. Identification and Characterization of Hypoxia-Regulated Endothelial Circular RNA. Circ Res. 2015;117(10):884-90.
75. Su H, Zou D, Sun Y, Dai Y. Hypoxia-associated circDENND2A promotes glioma aggressiveness by sponging miR-625-5p. Cell Mol Biol Lett. 2019;24:24.
76. Wang Y, Zhao R, Liu W, Wang Z, Rong J, Long X, et al. Exosomal circHIPK3 Released from Hypoxia-Pretreated Cardiomyocytes Regulates Oxidative Damage in Cardiac Microvascular Endothelial Cells via the miR-

29a/IGF-1 Pathway. Oxid Med Cell Longev. 2019;2019:7954657.
77. Lee S, Kopp F, Chang TC, Sataluri A, Chen B, Sivakumar S, et al. Noncoding RNA NORAD Regulates Genomic Stability by Sequestering PUMILIO Proteins. Cell. 2016;164(1-2):69-80.
78. Tripathi V, Ellis JD, Shen Z, Song DY, Pan Q, Watt AT, et al. The nuclear-retained noncoding RNA MALAT1 regulates alternative splicing by modulating SR splicing factor phosphorylation. Mol Cell. 2010;39(6):925-38.
79. Wahlestedt C. Targeting long non-coding RNA to therapeutically upregulate gene expression. Nat Rev Drug Discov. 2013;12(6):433-46.
80. Al Tameemi W, Dale TP, Al-Jumaily RMK, Forsyth NR. Hypoxia-Modified Cancer Cell Metabolism. Front Cell Dev Biol. 2019;7:4-.
81. Bavelloni A, Ramazzotti G, Poli A, Piazzi M, Focaccia E, Blalock W, et al. MiRNA-210: A Current Overview. Anticancer research. 2017;37(12):6511-21.
82. Tang T, Yang Z, Zhu Q, Wu Y, Sun K, Alahdal M, et al. Up-regulation of miR-210 induced by a hypoxic microenvironment promotes breast cancer stem cells metastasis, proliferation, and self-renewal by targeting E-cadherin. FASEB J. 2018:fj201801013R.
83. Yu Y, Min Z, Zhou Z, Linhong M, Tao R, Yan L, et al. Hypoxia-induced exosomes promote hepatocellular carcinoma proliferation and metastasis via miR-1273f transfer. Exp Cell Res. 2019:111649.
84. Takahashi K, Yan IK, Haga H, Patel T. Modulation of hypoxia-signaling pathways by extracellular linc-RoR. J Cell Sci. 2014;127.
85. Wozniak M, Peczek L, Czernek L, Duchler M. Analysis of the miRNA Profiles of Melanoma Exosomes Derived Under Normoxic and Hypoxic Culture Conditions. Anticancer research. 2017;37(12):6779-89.
86. Mittal V. Epithelial Mesenchymal Transition in Tumor Metastasis. Annual review of pathology. 2018;13:395-412.
87. Li Z, He F, Yang Z, Cao X, Dai S, Zou J, et al. Exosomal miR-25-3p derived from hypoxia tumor mediates IL-6 secretion and stimulates cell viability and migration in breast cancer. RSC Advances. 2019;9(3):1451-9.
88. Zhang X, Sai B, Wang F, Wang L, Wang Y, Zheng L, et al. Hypoxic BMSC-derived exosomal miRNAs promote metastasis of lung cancer cells via STAT3-induced EMT. Mol Cancer. 2019;18(1):40.
89. Doktorova H, Hrabeta J, Khalil MA, Eckschlager T. Hypoxia-induced chemoresistance in cancer cells: The role of not only HIF-1. Biomedical papers of the Medical Faculty of the University Palacky, Olomouc, Czechoslovakia. 2015;159(2):166-77.
90. Abraham J, Salama NN, Azab AK. The role of P-glycoprotein in drug resistance in multiple myeloma. Leuk Lymphoma. 2015;56(1):26-33.
91. Dong C, Liu X, Wang H, Li J, Dai L, Li J, et al. Hypoxic non-small-cell lung cancer cell-derived exosomal miR-21 promotes resistance of normoxic cell to cisplatin. Onco Targets Ther. 2019;12:1947-56.
92. Takahashi K, Yan IK, Kogure T, Haga H, Patel T. Extracellular vesicle-mediated transfer of long non-coding RNA ROR modulates chemosensitivity in human hepatocellular cancer. FEBS open bio. 2014;4:458-67.
93. Fang G, Liu J, Wang Q, Huang X, Yang R, Pang Y, et al. MicroRNA-

223-3p Regulates Ovarian Cancer Cell Proliferation and Invasion by Targeting SOX11 Expression. International journal of molecular sciences. 2017;18(6):1208.
94. Laios A, O'Toole S, Flavin R, Martin C, Kelly L, Ring M, et al. Potential role of miR-9 and miR-223 in recurrent ovarian cancer. Molecular Cancer. 2008;7(1):35.
95. Zhu X, Shen H, Yin X, Yang M, Wei H, Chen Q, et al. Macrophages derived exosomes deliver miR-223 to epithelial ovarian cancer cells to elicit a chemoresistant phenotype. Journal of experimental & clinical cancer research : CR. 2019;38(1):81.
96. Gonzalez H, Hagerling C, Werb Z. Roles of the immune system in cancer: from tumor initiation to metastatic progression. Genes & development. 2018;32(19-20):1267-84.
97. Rao Q, Zuo B, Lu Z, Gao X, You A, Wu C, et al. Tumor-derived exosomes elicit tumor suppression in murine hepatocellular carcinoma models and humans in vitro. Hepatology. 2016;64(2):456-72.
98. Ye SB, Li ZL, Luo DH, Huang BJ, Chen YS, Zhang XS, et al. Tumor-derived exosomes promote tumor progression and T-cell dysfunction through the regulation of enriched exosomal microRNAs in human nasopharyngeal carcinoma. Oncotarget. 2014;5(14):5439-52.
99. Ye SB, Zhang H, Cai TT, Liu YN, Ni JJ, He J, et al. Exosomal miR-24-3p impedes T-cell function by targeting FGF11 and serves as a potential prognostic biomarker for nasopharyngeal carcinoma. J Pathol. 2016;240.
100. Day CL, Kaufmann DE, Kiepiela P, Brown JA, Moodley ES, Reddy S, et al. PD-1 expression on HIV-specific T cells is associated with T-cell exhaustion and disease progression. Nature. 2006;443(7109):350-4.
101. Ostrand-Rosenberg S. Myeloid derived-suppressor cells: their role in cancer and obesity. Curr Opin Immunol. 2018;51:68-75.
102. Tesi RJ. MDSC; the Most Important Cell You Have Never Heard Of. Trends Pharmacol Sci. 2019;40(1):4-7.
103. Suetsuna F, Harata S, Yoshimura N. Influence of the ultrasonic surgical aspirator on the dura and spinal cord. An electrohistologic study. Spine (Phila Pa 1976). 1991;16(5):503-9.
104. Messmer MN, Netherby CS, Banik D, Abrams SI. Tumor-induced myeloid dysfunction and its implications for cancer immunotherapy. Cancer Immunol Immunother. 2015;64(1):1-13.
105. Li L, Cao B, Liang X, Lu S, Luo H, Wang Z, et al. Microenvironmental oxygen pressure orchestrates an anti- and pro-tumoral gammadelta T cell equilibrium via tumor-derived exosomes. Oncogene. 2019;38(15):2830-43.
106. Guo X, Qiu W, Liu Q, Qian M, Wang S, Zhang Z, et al. Immunosuppressive effects of hypoxia-induced glioma exosomes through myeloid-derived suppressor cells via the miR-10a/Rora and miR-21/Pten pathways. Oncogene. 2018;37.
107. Mills CD, Kincaid K, Alt JM, Heilman MJ, Hill AM. M-1/M-2 macrophages and the Th1/Th2 paradigm. J Immunol. 2000;164(12):6166-73.
108. Allavena P, Sica A, Garlanda C, Mantovani A. The Yin-Yang of

tumor-associated macrophages in neoplastic progression and immune surveillance. Immunol Rev. 2008;222:155-61.
109. Chen X, Zhou J, Li X, Wang X, Lin Y, Wang X. Exosomes derived from hypoxic epithelial ovarian cancer cells deliver microRNAs to macrophages and elicit a tumor-promoted phenotype. Cancer Lett. 2018;435:80-91.
110. Wang X, Luo G, Zhang K, Cao J, Huang C, Jiang T, et al. Hypoxic tumor-derived exosomal miR-301a mediates M2 macrophage polarization via PTEN/PI3Kgamma to promote pancreatic cancer metastasis. Cancer Res. 2018;78.
111. Park JE, Dutta B, Tse SW, Gupta N, Tan CF, Low JK, et al. Hypoxia-induced tumor exosomes promote M2-like macrophage polarization of infiltrating myeloid cells and microRNA-mediated metabolic shift. Oncogene. 2019;38(26):5158-73.
112. Viallard C, Larrivee B. Tumor angiogenesis and vascular normalization: alternative therapeutic targets. Angiogenesis. 2017;20(4):409-26.
113. Carmeliet P, Dor Y, Herbert JM, Fukumura D, Brusselmans K, Dewerchin M, et al. Role of HIF-1alpha in hypoxia-mediated apoptosis, cell proliferation and tumour angiogenesis. Nature. 1998;394(6692):485-90.
114. Mao G, Liu Y, Fang X, Liu Y, Fang L, Lin L, et al. Tumor-derived microRNA-494 promotes angiogenesis in non-small cell lung cancer. Angiogenesis. 2015;18(3):373-82.
115. Sruthi TV, Edatt L, Raji GR, Kunhiraman H, Shankar SS, Shankar V, et al. Horizontal transfer of miR-23a from hypoxic tumor cell colonies can induce angiogenesis. J Cell Physiol. 2018;233(4):3498-514.
116. Umezu T, Tadokoro H, Azuma K, Yoshizawa S, Ohyashiki K, Ohyashiki JH. Exosomal miR-135b shed from hypoxic multiple myeloma cells enhances angiogenesis by targeting factor-inhibiting HIF-1. Blood. 2014;124(25):3748-57.
117. Babayan A, Pantel K. Advances in liquid biopsy approaches for early detection and monitoring of cancer. Genome Med. 2018;10(1):21.
118. Palmirotta R, Lovero D, Cafforio P, Felici C, Mannavola F, Pelle E, et al. Liquid biopsy of cancer: a multimodal diagnostic tool in clinical oncology. Ther Adv Med Oncol. 2018;10:1758835918794630.
119. Bardelli A, Pantel K. Liquid Biopsies, What We Do Not Know (Yet). Cancer Cell. 2017;31(2):172-9.
120. Osti D, Del Bene M, Rappa G, Santos M, Matafora V, Richichi C, et al. Clinical Significance of Extracellular Vesicles in Plasma from Glioblastoma Patients. Clin Cancer Res. 2019;25(1):266-76.
121. Vasconcelos MH, Caires HR, Abols A, Xavier CPR, Line A. Extracellular vesicles as a novel source of biomarkers in liquid biopsies for monitoring cancer progression and drug resistance. Drug Resist Updat. 2019;47:100647.
122. Wang J, Zhou Y, Lu J, Sun Y, Xiao H, Liu M, et al. Combined detection of serum exosomal miR-21 and HOTAIR as diagnostic and prognostic biomarkers for laryngeal squamous cell carcinoma. Med Oncol. 2014;31(9):148.

123. Wang YH, Ji J, Wang BC, Chen H, Yang ZH, Wang K, et al. Tumor-Derived Exosomal Long Noncoding RNAs as Promising Diagnostic Biomarkers for Prostate Cancer. Cell Physiol Biochem. 2018;46(2):532-45.
124. Bjornetro T, Redalen KR, Meltzer S, Thusyanthan NS, Samiappan R, Jegerschold C, et al. An experimental strategy unveiling exosomal microRNAs 486-5p, 181a-5p and 30d-5p from hypoxic tumour cells as circulating indicators of high-risk rectal cancer. J Extracell Vesicles. 2019;8(1):1567219.
125. Pullan JE, Confeld MI, Osborn JK, Kim J, Sarkar K, Mallik S. Exosomes as Drug Carriers for Cancer Therapy. Mol Pharm. 2019;16(5):1789-98.
126. Kamerkar S, LeBleu VS, Sugimoto H, Yang S, Ruivo CF, Melo SA, et al. Exosomes facilitate therapeutic targeting of oncogenic KRAS in pancreatic cancer. Nature. 2017;546(7659):498-503.
127. Park HK, Ruterbusch JJ, Cote ML. Recent Trends in Ovarian Cancer Incidence and Relative Survival in the United States by Race/Ethnicity and Histologic Subtypes. Cancer Epidemiol Biomarkers Prev. 2017;26(10):1511-8.
128. Reid BM, Permuth JB, Sellers TA. Epidemiology of ovarian cancer: a review. Cancer Biol Med. 2017;14(1):9-32.
129. Buys SS, Partridge E, Black A, Johnson CC, Lamerato L, Isaacs C, et al. Effect of screening on ovarian cancer mortality: the Prostate, Lung, Colorectal and Ovarian (PLCO) Cancer Screening Randomized Controlled Trial. JAMA. 2011;305(22):2295-303.
130. Jacobs IJ, Menon U, Ryan A, Gentry-Maharaj A, Burnell M, Kalsi JK, et al. Ovarian cancer screening and mortality in the UK Collaborative Trial of Ovarian Cancer Screening (UKCTOCS): a randomised controlled trial. Lancet. 2016;387(10022):945-56.
131. Chang L, Ni J, Zhu Y, Pang B, Graham P, Zhang H, et al. Liquid biopsy in ovarian cancer: recent advances in circulating extracellular vesicle detection for early diagnosis and monitoring progression. Theranostics. 2019;9(14):4130-40.
132. Wang W, Han Y, Jo HA, Lee J, Song YS. Non-coding RNAs shuttled via exosomes reshape the hypoxic tumor microenvironment. J Hematol Oncol. 2020;13(1):67.
133. O'Brien K, Breyne K, Ughetto S, Laurent LC, Breakefield XO. RNA delivery by extracellular vesicles in mammalian cells and its applications. Nat Rev Mol Cell Biol. 2020;21(10):585-606.
134. McKenzie AJ, Hoshino D, Hong NH, Cha DJ, Franklin JL, Coffey RJ, et al. KRAS-MEK Signaling Controls Ago2 Sorting into Exosomes. Cell Rep. 2016;15(5):978-87.
135. Hagiwara K, Katsuda T, Gailhouste L, Kosaka N, Ochiya T. Commitment of Annexin A2 in recruitment of microRNAs into extracellular vesicles. FEBS Lett. 2015;589(24 Pt B):4071-8.
136. Otake K, Kamiguchi H, Hirozane Y. Identification of biomarkers for amyotrophic lateral sclerosis by comprehensive analysis of exosomal mRNAs in human cerebrospinal fluid. BMC Med Genomics. 2019;12(1):7.
137. Santangelo L, Giurato G, Cicchini C, Montaldo C, Mancone C,

Tarallo R, et al. The RNA-Binding Protein SYNCRIP Is a Component of the Hepatocyte Exosomal Machinery Controlling MicroRNA Sorting. Cell Rep. 2016;17(3):799-808.
138. Hobor F, Dallmann A, Ball NJ, Cicchini C, Battistelli C, Ogrodowicz RW, et al. A cryptic RNA-binding domain mediates Syncrip recognition and exosomal partitioning of miRNA targets. Nat Commun. 2018;9(1):831.
139. Eismann J, Hirschfeld M, Erbes T, Rucker G, Jager M, Ritter A, et al. Hypoxia- and acidosis-driven aberrations of secreted microRNAs in endometrial cancer in vitro. Oncol Rep. 2017;38(2):993-1004.
140. Hu W, Liu C, Bi ZY, Zhou Q, Zhang H, Li LL, et al. Comprehensive landscape of extracellular vesicle-derived RNAs in cancer initiation, progression, metastasis and cancer immunology. Mol Cancer. 2020;19(1):102.
141. Wang W, Im J, Kim S, Jang S, Han Y, Yang KM, et al. ROS-Induced SIRT2 Upregulation Contributes to Cisplatin Sensitivity in Ovarian Cancer. Antioxidants (Basel). 2020;9(11).
142. Kim S, Choi MC, Jeong JY, Hwang S, Jung SG, Joo WD, et al. Serum exosomal miRNA-145 and miRNA-200c as promising biomarkers for preoperative diagnosis of ovarian carcinomas. J Cancer. 2019;10(9):1958-67.
143. Kobayashi M, Sawada K, Nakamura K, Yoshimura A, Miyamoto M, Shimizu A, et al. Exosomal miR-1290 is a potential biomarker of high-grade serous ovarian carcinoma and can discriminate patients from those with malignancies of other histological types. J Ovarian Res. 2018;11(1):81.
144. Marton E, Lukacs J, Penyige A, Janka E, Hegedus L, Soltesz B, et al. Circulating epithelial-mesenchymal transition-associated miRNAs are promising biomarkers in ovarian cancer. J Biotechnol. 2019;297:58-65.
145. Todeschini P, Salviato E, Paracchini L, Ferracin M, Petrillo M, Zanotti L, et al. Circulating miRNA landscape identifies miR-1246 as promising diagnostic biomarker in high-grade serous ovarian carcinoma: A validation across two independent cohorts. Cancer Lett. 2017;388:320-7.
146. Zuberi M, Mir R, Khan I, Javid J, Guru SA, Bhat M, et al. The Promising Signatures of Circulating microRNA-145 in Epithelial Ovarian Cancer Patients. Microrna. 2020;9(1):49-57.
147. Tan DS, Agarwal R, Kaye SB. Mechanisms of transcoelomic metastasis in ovarian cancer. Lancet Oncol. 2006;7(11):925-34.
148. Kim S, Kim B, Song YS. Ascites modulates cancer cell behavior, contributing to tumor heterogeneity in ovarian cancer. Cancer Sci. 2016;107(9):1173-8.
149. Ford CE, Werner B, Hacker NF, Warton K. The untapped potential of ascites in ovarian cancer research and treatment. Br J Cancer. 2020;123(1):9-16.
150. Kim SI, Jung M, Dan K, Lee S, Lee C, Kim HS, et al. Proteomic Discovery of Biomarkers to Predict Prognosis of High-Grade Serous Ovarian Carcinoma. Cancers (Basel). 2020;12(4).
151. Andre-Gregoire G, Bidere N, Gavard J. Temozolomide affects Extracellular Vesicles Released by Glioblastoma Cells. Biochimie. 2018;155:11-5.

152. Arscott WT, Tandle AT, Zhao S, Shabason JE, Gordon IK, Schlaff CD, et al. Ionizing radiation and glioblastoma exosomes: implications in tumor biology and cell migration. Transl Oncol. 2013;6(6):638-48.
153. Drost J, Clevers H. Organoids in cancer research. Nat Rev Cancer. 2018;18(7):407-18.
154. Li J, Xu H, Zhang L, Song L, Feng D, Peng X, et al. Malignant ascites-derived organoid (MADO) cultures for gastric cancer in vitro modelling and drug screening. J Cancer Res Clin Oncol. 2019;145(11):2637-47.
155. Kim G, An HJ, Lee MJ, Song JY, Jeong JY, Lee JH, et al. Hsa-miR-1246 and hsa-miR-1290 are associated with stemness and invasiveness of non-small cell lung cancer. Lung Cancer. 2016;91:15-22.
156. Zhang WC, Chin TM, Yang H, Nga ME, Lunny DP, Lim EK, et al. Tumour-initiating cell-specific miR-1246 and miR-1290 expression converge to promote non-small cell lung cancer progression. Nat Commun. 2016;7:11702.
157. Xiao X, Yang D, Gong X, Mo D, Pan S, Xu J. miR-1290 promotes lung adenocarcinoma cell proliferation and invasion by targeting SOCS4. Oncotarget. 2018;9(15):11977-88.
158. Sakha S, Muramatsu T, Ueda K, Inazawa J. Exosomal microRNA miR-1246 induces cell motility and invasion through the regulation of DENND2D in oral squamous cell carcinoma. Sci Rep-Uk. 2016;6.
159. Li XJ, Ren ZJ, Tang JH, Yu Q. Exosomal MicroRNA MiR-1246 Promotes Cell Proliferation, Invasion and Drug Resistance by Targeting CCNG2 in Breast Cancer. Cell Physiol Biochem. 2017;44(5):1741-8.
160. Huang J, Shen M, Yan M, Cui Y, Gao Z, Meng X. Exosome-mediated transfer of miR-1290 promotes cell proliferation and invasion in gastric cancer via NKD1. Acta Biochim Biophys Sin (Shanghai). 2019;51(9):900-7.
161. Mao Y, Liu J, Zhang D, Li B. MiR-1290 promotes cancer progression by targeting nuclear factor I/X(NFIX) in esophageal squamous cell carcinoma (ESCC). Biomed Pharmacother. 2015;76:82-93.
162. Ta N, Huang X, Zheng K, Zhang Y, Gao Y, Deng L, et al. miRNA-1290 Promotes Aggressiveness in Pancreatic Ductal Adenocarcinoma by Targeting IKK1. Cell Physiol Biochem. 2018;51(2):711-28.
163. Qian M, Wang S, Guo X, Wang J, Zhang Z, Qiu W, et al. Hypoxic glioma-derived exosomes deliver microRNA-1246 to induce M2 macrophage polarization by targeting TERF2IP via the STAT3 and NF-kappaB pathways. Oncogene. 2020;39(2):428-42.
164. Walbrecq G, Lecha O, Gaigneaux A, Fougeras MR, Philippidou D, Margue C, et al. Hypoxia-Induced Adaptations of miRNomes and Proteomes in Melanoma Cells and Their Secreted Extracellular Vesicles. Cancers (Basel). 2020;12(3).
165. Du J, Xu R. RORalpha, a potential tumor suppressor and therapeutic target of breast cancer. Int J Mol Sci. 2012;13(12):15755-66.
166. Jiang Y, Zhou J, Zhao J, Hou D, Zhang H, Li L, et al. MiR-18a-downregulated RORA inhibits the proliferation and tumorigenesis of glioma using the TNF-alpha-mediated NF-kappaB signaling pathway. EBioMedicine. 2020;52:102651.

167. Zheng X, Wu K, Liao S, Pan Y, Sun Y, Chen X, et al. MicroRNA-transcription factor network analysis reveals miRNAs cooperatively suppress RORA in oral squamous cell carcinoma. Oncogenesis. 2018;7(10):79.
168. Mattes J, Collison A, Foster PS. Emerging role of microRNAs in disease pathogenesis and strategies for therapeutic modulation. Curr Opin Mol Ther. 2008;10(2):150-7.
169. Aquino-Jarquin G. Emerging Role of CRISPR/Cas9 Technology for MicroRNAs Editing in Cancer Research. Cancer Res. 2017;77(24):6812-7.
170. Reda El Sayed S, Cristante J, Guyon L, Denis J, Chabre O, Cherradi N. MicroRNA Therapeutics in Cancer: Current Advances and Challenges. Cancers (Basel). 2021;13(11).
171. Cubillos-Ruiz JR, Baird JR, Tesone AJ, Rutkowski MR, Scarlett UK, Camposeco-Jacobs AL, et al. Reprogramming tumor-associated dendritic cells in vivo using miRNA mimetics triggers protective immunity against ovarian cancer. Cancer Res. 2012;72(7):1683-93.
172. Dwivedi SK, Mustafi SB, Mangala LS, Jiang D, Pradeep S, Rodriguez-Aguayo C, et al. Therapeutic evaluation of microRNA-15a and microRNA-16 in ovarian cancer. Oncotarget. 2016;7(12):15093-104.
173. Kafshdooz L, Pourfathi H, Akbarzadeh A, Kafshdooz T, Razban Z, Sheervalilou R, et al. The role of microRNAs and nanoparticles in ovarian cancer: a review. Artif Cells Nanomed Biotechnol. 2018;46(sup2):241-7.
174. Bertucci A, Kim KH, Kang J, Zuidema JM, Lee SH, Kwon EJ, et al. Tumor-Targeting, MicroRNA-Silencing Porous Silicon Nanoparticles for Ovarian Cancer Therapy. ACS Appl Mater Interfaces. 2019;11(27):23926-37.

초록

난소암은 초기 진단용 바이오마커의 부재로 대부분의 환자는 병변이 진행된 단계에서 진단된다. 일반적인 난소암의 전이 패턴은 악성 복수가 형성되는 복막전이를 특징으로 한다. 세포외 소포체(EV)는 액체 생검에서 유망한 임상 생체 지표로 떠오르고 있다. 본 연구에서는 난소암 진단 및 전이 조절을 위한 액체 생검 기반 EV miRNA 바이오마커를 발굴하는 것을 목표로 했다. EV 는 양성 부인과 질환 환자로부터 얻은 양성 복수및 혈장과 난소암 환자의 악성 복수및 혈장으로부터 분리되었다. 복수 및 혈장 유래 EV 의 miRNA 프로파일링을 조사하기 위해 small RNA 시퀀싱을 수행했다. 난소암 진단 시그니처 개발을 위해 복수와 혈장에서 공통적으로 발현 차이가 나는 miRNA 를 분석했고, 최종적으로 8 개의 miRNA(miR-1246, miR-1290, miR-483, miR-429, miR-34b-3p, miR-34c-5p, miR-145-5p, miR-449a)가 선택되었다. 8 개의 miRNA 를 이용한 난소암 EV miRNA (OCEM) 진단 시그니처는 본 연구내 데이터 세트에서 높은 진단 정확도를 보여주었다. (복수 서브셋: AUC=1; 혈장 서브셋: AUC=0.9375). 더 나아가, OCEM 진단 시그니처의 임상 사용 가능성을 확인하기 위해 다양한 임상 샘플(혈액, 조직 및 소변)이 포함된 여러 공개 데이터 세트를 이용해 평가했다. 그 결과 본 연구에서 발굴된 OCEM 진단 시그니처는 다양한 임상 샘플에서도 높은 진단 정확도를 보여주었다. 또한 악성 복수 유래 EV 가 난소암세포의 전이능에

미치는 영향도 조사했다. 그 결과 악성 복수유래 EV 가 난소암세포의 전이능을 크게 증가시키는 것으로 확인되었다. 특히, 악성 복수 유래 EV 에 의해 전달되는 miR-1246 과 miR-1290 은 공통 타겟 RORα를 조절하여 난소암 세포의 침입과 이동을 촉진하는 것으로 확인되었다.

본 연구는 액체 생검 전략으로서 EV miRNA 시그니처가 난소암 진단을 위해 임상적으로 적용할 수 있는 가능성을 시사한다. 또한 난소암 환자 복수 유래 EV 는 miRNA 의 전달을 통해 암 전이능을 크게 촉진할 수 있어 이는 잠재적인 난소암 치료 타겟으로의 사용이 기대된다.

주요어: 난소암, 세포외소포체, miRNAs, 복수, 액체 생검, 진단, 전이

학번: 2018-36129